Journal of South American Earth Sciences xxx (xxxx) xxx

Contents lists available at ScienceDirect

Journal of South American Earth Sciences

journal homepage: www.elsevier.com/locate/jsames

Constraining late paleozoic ice extent in the Paganzo basin of western Argentina: Provenance of the lower Paganzo group strata

Kathryn N. Pauls [a,*], John L. Isbell [a], C. Oscar Limarino [b], Pablo J. Alonso-Murauga [b], David H. Malone [c], L. Jazmin Schencman [b], Carina E. Colombi [d], Levi D. Moxness [e]

[a] University of Wisconsin-Milwaukee, 3209 N. Maryland Ave., Milwaukee, WI, 53211, USA
[b] Universidad de Buenos Aires-IGEBA (UBA-CONICET), Facultad de Ciencias Exactas y Naturales, Departamento de Ciencias Geológicas, Ciudad Universitaria Pab. 2, 1° Piso, CABA, Argentina
[c] Department of Geography, Geology and the Environment, Illinois State University, Normal, IL, 61790-4400, USA
[d] Instituto y Museo de Ciencias Naturales, Universidad Nacional de San Juan, Centro de Investigaciones de la Geosfera y la Biosfera - Conicet, España 400 (Norte), San Juan, Argentina
[e] North Dakota Geological Survey, 600 East Boulevard, Dept. 405, Bismarck, ND 58505-0840, USA

A B S T R A C T

The western margin of Gondwana records evidence of mid-Carboniferous glaciation (Visean- Bashkirian) in the strata of the Paganzo Basin and adjacent areas. Previous studies focused on constraining the orientations of ice flow and generalizing the extent and occurrence of glacial ice in the basin. However, there is uncertainty occurs concerning the location and extent of glaciation and the locations of glacial centers during deposition of the Guandacol Formation located in the western portion and the time correlative Malanzán Formation in the eastern parts of the basin respectively. Understanding these strata and the conditions that led to the deposition of these strata has important implications for understanding glaciation extent along the western margin of Gondwana during the late Paleozoic ice age. To refine the glaciation history, we present new paleocurrent, facies, and a comparative analysis of previously published and one new detrital zircon geochronology data set. Together, these data provide new insight into sediment dispersal patterns and glacial centers within the basin. Our data indicate that both units were deposited under cold climatic conditions that occurred across the entire basin, but that glaciers were restricted to the western portion of the basin. The facies analysis for both formations indicates very different depositional environments for the two units: glacial and glaciomarine environments in the west and non-glacial alluvial, alluvial fan and lacustrine and/or marine environments in the east. Detrital zircon geochronology indicates separate localized provenance signatures for the two formations. Furthermore, the detrital zircon populations allude to disconnected depositional centers. At Huaco, glacial flow in the Guandacol is oriented toward the northwest (i.e. 313°) and appears to be draining from an uplift that contains similar zircon age populations as the Sierra de Valle Fértil and Sierra de Pie de Palo ranges. In the Olta-Malanzán paleovalley system, drainage was off valley walls and down the valley axis (i.e. south and southwest) within the Sierras de Chepes region with limited sediment sourced from the east just beyond the paleovalley system. Paleoflow measurements reported from other known glacial localities along the western portion of the basin reflect a radial flow pattern within and away from deeply incised valleys that clearly point to upland glacial centers within the Cuyania and Precordilleran terranes.

1. Introduction

Over the past several decades, research on the late Paleozoic ice age (LPIA; 372-259 million years ago) has led to a better understanding of the development and termination of glaciation(s) across Gondwana. The LPIA is the only example of when a vegetated and biologically complex Earth shifted from an icehouse to a greenhouse state (Gastaldo et al., 1996; Montañez et al., 2007, 2016; Fielding et al., 2008a; Isbell et al., 2012; Montañez and Poulsen, 2013). Therefore, further research on the LPIA will help in understanding drivers that influence changing climatic regimes.

In the Paganzo Basin, located along the Panthallassan margin of western Argentina, glaciers developed during the Middle Mississippian (Visean) and disappeared in the early Pennsylvanian (Bashkirian; López-Gamundí et al., 1994; López-Gamundí, 1997; Limarino et al., 2002a, 2002b, 2014; Holz et al., 2008; Caputo et al., 2008; Henry et al., 2008, 2010; Isbell et al., 2012). However, other places in Gondwana at similar paleo-latitudes (e.g. southern Paraná Basin in Brazil) persisted until the end of the Carboniferous (based on facies changes and U–Pb radioisotopic ages; cf. Caputo and Crowell, 1985; Rocha Campos et al.,

* Corresponding author: University of Wisconsin-Milwaukee, 3209 N. Maryland Ave., Milwaukee, WI, 53211, USA.
E-mail addresses: kpauls@uwm.edu, kate.n.pauls@gmail.com (K.N. Pauls), jisbell@uwm.edu (J.L. Isbell), limar@gl.fcen.uba.ar (C.O. Limarino), pablo@gl.fcen.uba.ar (P.J. Alonso-Murauga), dhmalone@ilstu.edu (D.H. Malone), jazminsch@gmail.com (L.J. Schencman), ccolombi@unsj.edu.ar (C.E. Colombi), ldmoxness@gmail.com (L.D. Moxness).

https://doi.org/10.1016/j.jsames.2020.102899
Received 31 May 2020; Received in revised form 11 September 2020; Accepted 11 September 2020
Available online 25 September 2020

2008; Isbell et al., 2012; Griffis et al., 2018), or perhaps until the Early Permian (i.e. early Cisuralian, eastern Paraná Basin based on palynomorphic assemblages; cf. Mottin et al., 2018). In order to better refine the understanding of the nature and location of glaciation, as well as the timing of the disappearance of glaciers along the western margin of Gondwana, we used paleoenvironmental, paleocurrent, and geochronological information. We 1) examined published and new evidence for glaciers using paleoflow and facies analyses; 2) compared published and one new data set of detrital zircon age populations the lowermost Panganzo Group strata from two locations within the Paganzo Basin to assess provenance; 3) used this data to test various hypotheses regarding the extent and location of ice centers within the basin; and 4) evaluated and discussed the current understanding of the location, timing and extent of the uplands within and surrounding the basin during the early-middle Carboniferous.

2. Background

Western Argentina contains evidence of glaciation during the LPIA (Visean to early Bashkirian), concentrated within several basins along the Panthalassan margin. Following Limarino et al. (2002b) and Marenssi et al. (2005), these basins can be broken into paleogeographic domains of open marine, transitional and continental dominated basin settings. The Paganzo Basin incorporates two of these settings: transitional and continental-dominated. This basin, which spans an area of approximately 144,000 km^2 at its largest extent, is bounded today by the Sierras Pampeanas to the east, north and south, and the Precordilleran range in the west. The development and structure of the Paganzo Basin is still under debate. Various studies identified it as a retroarc foreland basin (Ramos et al., 1988), a rift basin (Astini et al., 1995, 2009; Astini, 2010), or as a pull-apart basin due to strike-slip activity along the Panthalassan margin of Gondwana (Limarino et al., 2002a, 2014; Milana and di Pasquo, 2019). Regardless of the exact type of basin, it was a major catchment for late Paleozoic sediments, and records early evidence of glaciation during the peak Mid-Carboniferous phase of the LPIA.

This evidence is recorded at the base of the late Paleozoic strata of the Paganzo Basin, which contains both ice-proximal and subglacial deposits (López-Gamundí, 1987; Limarino and Gutiérrez, 1990; Net, 1999; López-Gamundí and Martinez, 2000; Limarino et al., 2002b, 2014; Henry, 2007; Henry et al., 2008, 2010; César et al., 2011; Alonso--Muruaga et al., 2018; Valdez Buso et al., 2017, 2020). The Paganzo Group strata cover the entire basin and are broken up into regional formations (Fig. 1). The basal part of the Paganzo Group is the subject of this paper. In the west, the glacigenic units are known as the Jejenes and the Guandacol formations, in the central portion of the basin, this unit is referred to as the Lagares Formation, and in the east the Malanzán Formation is the time-equivalent unit (Limarino et al., 2002a, 2006). The various formations are correlated using palynological and fossil plant remains, as well as some radiometric ages determined from strata in the western Paganzo and Río Blanco basins (cf. Gulbranson et al., 2010, 2015; César et al., 2011, 2019; Valdez Buso et al., 2020). The correlations between these units, and previous interpretations of these deposits as glacial in origin, has provided grounds for a few hypotheses concerning the extent of glaciation during the Visean and Bashkirian stages in the Paganzo Basin. One of the goals of this study is to test hypotheses on the extent of glaciation in the basin (Fig. 2). There are two main hypotheses concerning the distribution and style of glaciation within the Paganzo Basin region, as portrayed in Fig. 2B and C.

One such hypothesis, as demonstrated in Fig. 2B, maintains that there were several potentially separate glacial centers in the basin. In the western domain, there was a glaciated upland in the Precordilleran region of the western Sierras Pampeanas, known as the Protoprecordillera (cf. proto-Precordillera of Amos and Rolleri, 1965; González, 1975, Fig. 2A). This region is a small terrane that was uplifted as a fold-and-thrust belt during the Chañic orogeny (middle Devonian to earliest Mississippian), which occurred due to the accretion of the Chilenia terrane to Gondwana (Ramos et al., 1984, 1986; López-Gamundí et al., 1994; Limarino et al., 2006, 2014; Henry et al., 2008; Isbell et al., 2012; Moxness et al., 2018). The Protoprecordilleran range is considered by certain studies to be an ancient mountain belt and significant paleotopographic high that developed from the fold-and-thrust belt, and today underlies the present Precordilleran range of the Andes Mountains (González Bonorino, 1975; Ramos, 1988; López-Gamundí et al., 1994; Limarino et al., 2002, 2006; Isbell et al., 2012). Glaciomarine deposition occurred during the Visean-early Bashkirian in deeply-incised paleovalleys that emanated from the Protoprecordilleran region (Fig. 2A) and into the surrounding Paganzo, Calingasta-Uspallata and Rio Blanco basins (cf. López-Gamundí et al., 1997; Limarino et al., 2002a, 2002b, 2006; Kneller et al., 2004; Dykstra et al., 2006, 2007; Limarino and Spalletti, 2006; Henry, 2007; Henry et al., 2008, 2010; Astini, 2010; Gulbranson et al., 2010; César et al., 2011; Isbell et al., 2012; Aquino et al., 2014; Alonso-Muruaga et al., 2018). The diamictites at the base of the Lagares Formation in the central Paganzo Basin at least indicate a potential for glacial influence along the proto-Famatina arch (Fig. 2B; Limarino et al., 2002a, 2006; Limarino and Spalletti, 2006; Astini, 2010; Tedesco et al., 2010; Limarino et al., 2014). There are also reported diamictites in the eastern part of the Paganzo Basin within the Sierra de Chepes region (Locality 2 in Fig. 2), at the base of the Malanzán Formation, which contain outsized clasts and sparse debris flows, but these diamictites lack the traditional characteristics of true subglacial and proglacial deposits, such as faceted and striated clasts and the occurrence of sheared horizons (Andreis et al., 1986; Sterren and Martínez, 1996; Socha et al., 2014; Limarino et al., 2014; Moxness et al., 2018). Nevertheless, the presence of diamictites has led to the interpretation of glaciation throughout the Paganzo Basin, but in the form of more localized alpine glaciation centered on the various ancient highlands (Fig. 2B).

A second hypothesis, demonstrated in Fig. 2C, contends that there was extensive regional uplift for this region during the Devonian and earliest Carboniferous (340-325 Ma; Astini, 2009; Astini et al., 2010), followed by an extensive peneplain (Jordan et al., 1989). In this scenario, the Protoprecordillera was not a significant uplift, and therefore did not host glacial ice centers. The peneplain surface in the Paganzo Basin region was instead thought to have been formed by a large ice sheet that was centered in the eastern Sierras Pampeanas, or on the Pampean arch (Milana and Berscowski, 1987, 1990, 1993; Milana,

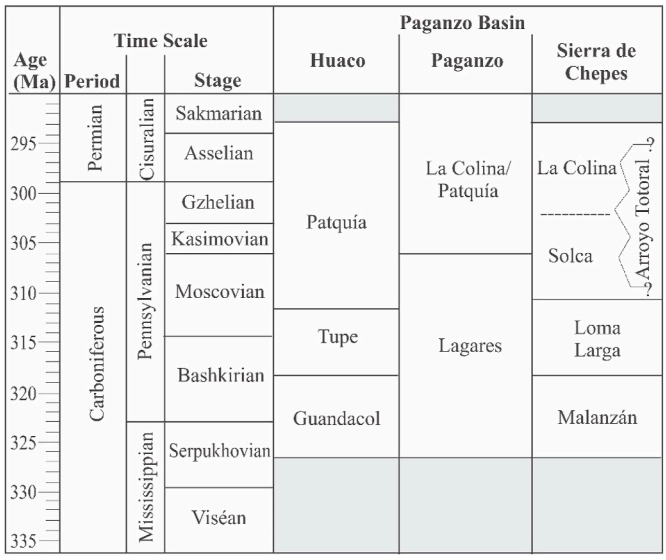

Fig. 1. Correlation chart for the late Paleozoic Paganzo Group strata for the sites in the Paganzo Basin, Argentina mentioned in the text. Ages and units are based on Limarino et al. (2002a, 2002b, 2006, 2014), César et al. (2011, 2019).

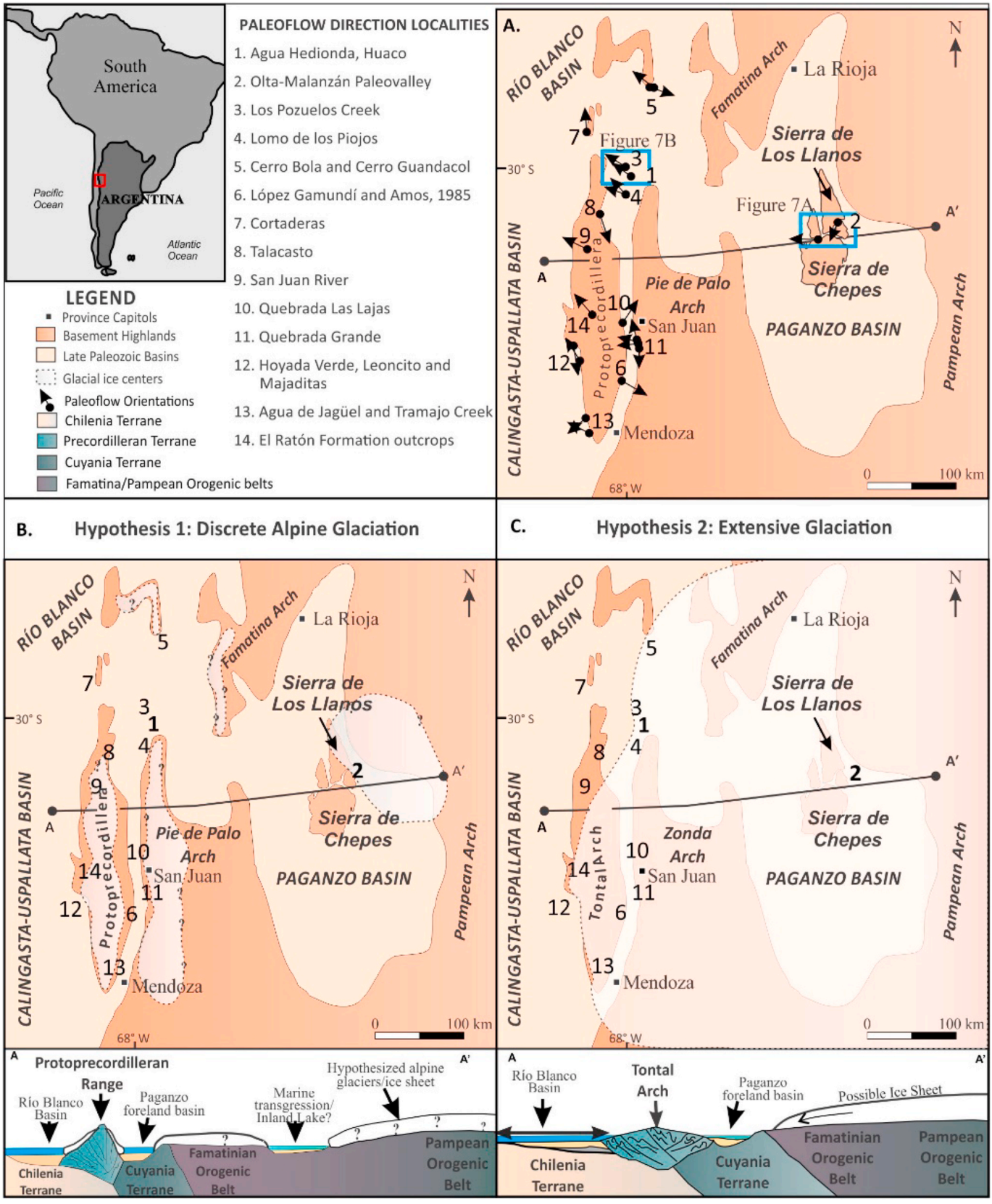

(caption on next page)

Fig. 2. A. Map of the Paganzo Basin during the late Paleozoic with arrows indicating paleoflow measurements from numerous publications, modified from Henry et al. (2008). Paleoflow data are from the following list of papers: (1) Agua Hedionda, Huaco - Bossi and Andreis (1981), Marenssi et al. (2002, 2005), López Gamundí and Martínez (2000), this study (2) Olta-Malanzán Paleovalley - Andreis et al. (1986), this study (3) Los Pozuelos Creek - Marenssi et al. (2005) (4) Loma de Los Piojos - López Gamundí and Martínez (2000), Alonso-Muruaga et al. (2012) (5) Cerro Bola, Cerro Guandacol - Andreis et al. (1975), López Gamundí et al. (1994), Dykstra et al. (2011), Fallgatter et al. (2019; (6) López Gamundí and Amos (1985), López Gamundí et al. (1994) (7) Cortaderas - Scalabrini Ortiz (1972), López Gamundí et al. (1994), Henry et al. (2010) (8) Talacasto - Aquino et al. (2014) (9) Henry et al. (2008) (10) Dykstra et al. (2006, 2007) (11) Quebrada Grande - Kneller et al. (2004), Dykstra et al. (2006), Valdez Buso et al. (2017), Fallgatter et al. (2019) (12) Hoyada Verde, Leoncito, Majaditas - González (1981), López Gamundí (1984); López Gamundí et al. (1994); López Gamundí and Martínez (2000, 2003); this study (13) Agua de Jagüel and Tramajo Creek - López Gamundí (1984), López Gamundí et al. (1994), Henry et al. (2008, 2010); this study (14) El Ratón Formation - López Gamundí et al. (1994). B. A plan-view and a cross-sectional view of discrete alpine glacial centers found throughout the Paganzo Basin (cf. Limarino et al., 2002a, 2006; 2014; Henry et al., 2008; Isbell et al., 2012). C. Extensive glaciation from an ice sheet centered in the Eastern Sierras Pampeanas that covered, and then drained through the uplands across the Paganzo Basin (cf. Valdez Buso et al., 2017; Milana and Bercowski, 1987, 1990; 1993; Milana, 1988; Milana et al., 1987; Aquino et al., 2014). Modified after Henry et al. (2008) and Moxness et al. (2018).

1988; Milana et al., 1987; Astini, 2010; Aquino et al., 2014; Valdez Buso et al., 2017, 2020; Milana and di Pasquo, 2019). This ice sheet would have advanced across the uplands, and as the ice sheet collapsed, it carved through a chain of uplands that was known as the Zonda and Tontal arches in the west, as well as the Sierras de Chepes region in the east (Fig. 6C). These uplands were dissected by glacial valleys that drained the ice sheet and deposited the glacigenic strata of the Paganzo Group (i.e. the Guandacol, Lagares and Malanzán formations). This paper will test these hypotheses to better determine the mid-Carboniferous glacial history of the western margin of Gondwana.

3. Regional geologic setting

The western margin of Argentine Gondwana is an assemblage of terranes (the Pampia, Precordillera and Chilenia terranes), igneous intrusions, and subsequent metamorphosed units (Ramos, 1988, 1999; Pankhurst et al., 1998; Ramos et al., 1998, 2010; 2015; Rapela et al., 1998, 2008; Rapalini, 2005; Dahlquist et al., 2010; Einhorn et al., 2015). The resulting paleotopographic highs created terrane accretion have been implicated in the climate and depositional histories of the subsequent basins (cf. Limarino et al., 2002a, 2002b, 2006).

The Sierras Pampeanas today make up most of the highlands between the Precordillera terrane and the Rio de la Plata craton and are divided into magmatic belts that correspond to different accretionary events of western Argentina (Fig. 2B and C). The easternmost Sierras Pampeanas were formed during the Cambrian as the Pampia terrane docked to the Rio de La Plata craton, and therefore contain zircon ages between 500 and 600 Ma (Rapela et al., 1998, 2007; Ramos et al., 2015). The ranges include the Sierra de Córdoba, Sierra del norte de Córdoba, Sierra Ambato, Sierra Ancasti and others (Rapela et al., 1998; Leal et al., 2003; Llambías et al., 2003; Toselli et al., 2003).

The Sierras Pampeanas also include the Ordovician Famatina magmatic belt (490-450 Ma, with the main magmatism occurring between 490 and 470 Ma) and the eastern portion of the Cuyania Terrane (Pankhurst et al., 1998, 2000; Ramos et al., 1998; Keller, 1999; Ramos, 1999). The Famatina orogenic belt runs north-south between the Pampean orogenic belt and the Cuyania composite terrane, and encompasses Sierra de Valle Fértil, Sierras Famatina, Sierra de San Luis, and the Sierras de Chepes, Los Llanos, and Malanzán (Pankhurst et al., 1998, 2000; Toselli et al., 2003; Vujovich and Ostera, 2003; Dahlquist et al., 2010; Einhorn et al., 2015). The Sierras de Chepes region contains crystallization ages from 477 to 497 Ma (Pankhurst et al., 1998; Stuart-Smith et al., 1999; Enkelmann et al., 2014). The western Famatina belt was also subject to metamorphism around 469 Ma, and contains some younger ages north of the Sierra de Valle Fértil region (Pankhurst et al., 1998, 2000; Ramos et al., 1998, 2010; 2015; Rapela et al., 1998, 2001; Rapalini, 2005; Dahlquist et al., 2010; Einhorn et al., 2015). Additionally, these Ordovician granites were intruded by post-orogenic granitic bodies during the Devonian-early Carboniferous (365-345 Ma; Dahlquist et al., 2010; Martina et al., 2018).

The Cuyania terrane is a microplate that either rifted from another region of Gondwana or rifted from Laurentia during the Cambrian or earliest Ordovician (Kay et al., 1996; Keller et al., 1998; Keller, 1999; Ramos, 2000; Casquet et al., 2001, 2012; Willner et al., 2008). The Cuyania terrane accreted to the western margin of Gondwana around 460-435 Ma, and contains sedimentary packages of "Grenville-age" (1165-980 Ma) and occur in the western Sierras Pampeanas ranges of the Sierra de Pie de Palo and the Sierras de Umango, Maz and Espinol (Huff et al., 1998; Ottone et al., 2001; Dahlquist et al., 2010; Sial et al., 2013; Verdecchia et al., 2014, 2018). Superimposed upon Cuyania is a fold-and-thrust belt that is known as the Precordillera terrane, which contains Cambrian-Ordovician sedimentary units (i.e. the San Juan Limestone and Los Azules Formation) that represent carbonate and siliciclastic platform depositional environments (Kay et al., 1996; Huff et al., 1998; Keller et al., 1998; Keller, 1999; Ottone et al., 2001; Willner et al., 2008). The Precordillera terrane is interpreted to be part of a tectonic belt that made up either the proto-Precordilleran range or the Tontal Arch during the early Carboniferous (cf. Amos and Rolleri, 1965; Limarino et al., 2006; Aquino et al., 2014; Valdez Buso et al., 2017, 2020). The Cambrian and Ordovician deposits of the Precordillera and Cuyania terranes are overlain conformably or unconformably by sedimentary packages that range in age from Silurian to Triassic (cf. Keller et al., 1998; Keller, 1999; Willner et al., 2008).

3.1. Geology of the lower Paganzo Group strata

Purported glacial deposits of the Paganzo Group strata are reported all throughout the Paganzo Basin and are interpreted to be mostly fjord-like or glacial valley environments (Marenssi et al., 2005; Limarino et al., 2002a, 2002b, 2014; Aquino et al., 2014; Valdez Buso et al., 2017; Alonso-Muruaga et al., 2018; Fallgatter et al., 2019; Milana and di Pasquo, 2019). In this study, we measured detailed stratigraphic sections at two localities on the western (Huaco locality) and eastern (i.e. the Olta-Malanzán paleovalley) margins of the Paganzo Basin for an evaluation of the extent of glacial deposits within the basin (Fig. 3A and B). While much is known about the glacial deposits of the Paganzo Group strata, new understandings of the climate and depositional environments across the basin have come to light (cf. Valdez Buso et al., 2017, 2020; Alonso-Muruaga et al., 2018; Moxness et al., 2018; Pauls et al., 2019; Fallgatter et al., 2019; Milana and di Pasquo, 2019). Recent studies suggest that glacial strata may not be present throughout the basin (cf. Moxness et al., 2018; Pauls et al., 2019). To evaluate the interconnection between the eastern and western margins of the basin and to refine the extent of glaciation, we present lithofacies analyses and detrital zircon geochronology results from the Malanzán Formation of the Olta-Malanzán region in the eastern Paganzo Basin and from the Guandacol Formation at Huaco on the western margin (Fig. 3).

3.2. Olta-Malanzán paleovalley

The Olta-Malanzán paleovalley (OMPV) occurs in an isolated uplift of the Famatina orogenic belt of the Sierras Pampeanas (Fig. 3A). The paleovalley developed in an alpine or mountain valley setting, either carved by glacial ice (cf. Sterren and Martinez, 1996; Enkelmann et al.,

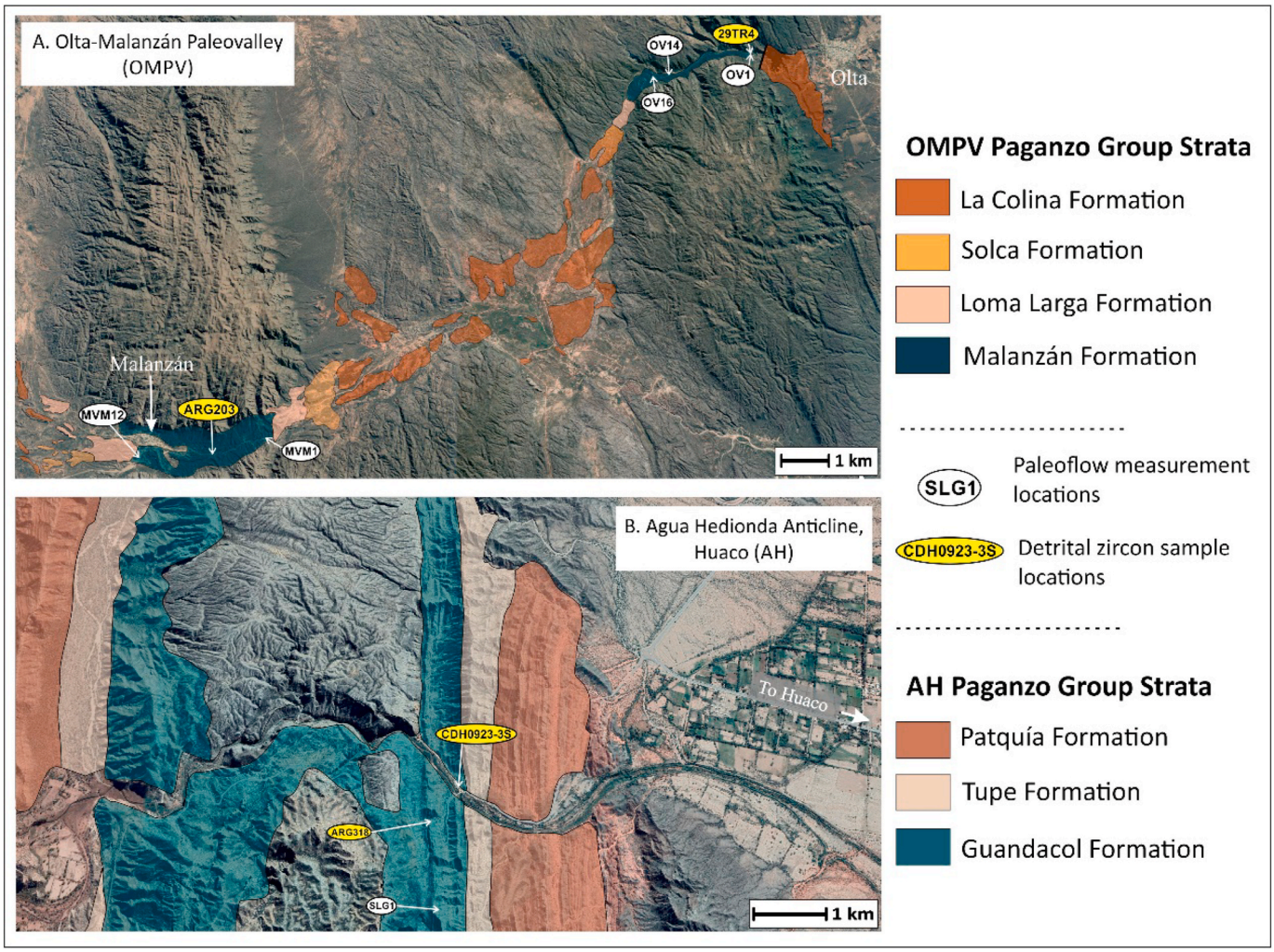

Fig. 3. Google Earth aerial image with the geologic units of the Paganzo Group mapped showing the locations of the paleoflow measurements (white ellipsoids) and detrital zircon samples (yellow ellipsoids). A. The Olta-Malanzán paleovalley system (OMPV) with the Malanzán, Loma Larga, Solca, and La Colina formations (Andreis et al., 1986; Limarino et al., 2014; Moxness et al., 2018; Pauls et al., 2019). Detrital zircon simple ARG203 is from Craddock et al. (2019), and sample 29TR4 is from Enkelmann et al. (2014). B. The Agua Hedionda anticline, near the town of Huaco with the Guandacol, Tupe and Patquía formations. Mapped units are from Marenssi et al. (2002). Detrital zircon sample ARG318 is from Craddock et al. (2019), and sample CDH0923-3 S is from this study. (For interpretation of the references to colour in this figure legend, the reader is referred to the Web version of this article.)

2014; Rabassa et al., 2014; Socha et al., 2014) or formed as the result of a fault-bounded basin (Bracaccini, 1948; Andreis et al., 1986; Buatois and Mangano, 1995; Net and Limarino, 1999; Moxness et al., 2018). The Paleozoic valley fill overlies various granitic-granodioritic and metamorphic complexes (the Chepes granodiorite, Tuaní and Asperezas granite suites, and the Olta schist and phyllite). The paleovalley is ~40 km long and trends northeast-southwest between the towns of Olta (northeastern end) and Malanzán (southwestern end). The paleovalley ranges from 500 to 5500 m in width and widens to the southwest. The Río Olta drains this paleovalley to the east, but paleocurrent data from the Paganzo Group strata indicate a westerly drainage during the late Paleozoic. The paleovalley is exposed in a syncline, with the oldest (i.e. Serpukhovian-Bashkirian) material at the easternmost and westernmost ends, and the youngest (i.e. Permian) strata exposed toward the center (Fig. 3A). Therefore, the paleovalley is often divided into two segments, the Olta paleovalley (OPV) to the northeast and the Malanzán paleovalley (MPV) to the southwest. The Malanzán Formation is the basal unit of the Paganzo Group in the paleovalley system and is the strata of interest for this study (Bracaccini, 1948; Azcuy, 1975; Andreis et al., 1986; Azcuy et al., 1987; Buatois and Mángano, 1995; Sterren and Martinez, 1996; Azcuy et al., 1987; Net and Limarino, 1999; Gutiérrez and Limarino, 2001; Net et al., 2002).

3.3. Huaco locality

Strata of the Guandacol Formation are exposed on either flank of the Agua Hedionda (AH) anticline, near the city of Huaco (cf. Bossi and Andreis, 1985; López-Gamundí et al., 1994; Martínez, 1993; López-Gamundí and Martínez, 2000; Pazos, 2000, 2002a; 2002b; Marenssi et al., 2002; Limarino et al., 2002a; Marenssi et al., 2005). Sections were measured at Cuesta de Huaco, along the eastern flank of the anticline, north and south of the Huaco River and Route 40 (Fig. 3B). Strata were measured here as this section represents one of the most complete records of late Paleozoic strata in northwestern Argentina. The Guandacol Formation overlies the Ordovician San Juan Formation, which serves as the basement for the area. Multiple studies at the Cuesta de Huaco and Los Pozuelos Creek localities have interpreted this area as a fjord setting containing advance and retreat cycles, that is succeeded by a final glacial withdrawal, and a transition to deltaic settings (López-Gamundí and Martínez, 2000; Pazos, 2000, 2002a, 2002b; Marenssi et al., 2002; Limarino et al., 2002).

4. Methods

4.1. Lithofacies and paleocurrent analyses methods

Field work was conducted in March 2015, August 2016 and August 2017 and used standard stratigraphic and sedimentological techniques to examine and measure 24 sections of the Malanzán Formation and seven sections of the Guandacol Formation. Poorly sorted clastic material was identified using the classification scheme developed by Hambrey and Glasser (2012). Careful attention was paid to the presence and absence of striated pavements and striated clasts, and the characteristics of diamictites and conglomerates. Facies distribution was accomplished by extensive mapping at both localities. To track changes in sediment dispersal and transport direction through time, paleoflow and paleocurrent measurements were taken at multiple levels within the Malanzán and Gundacol formations. Paleoflow and paleoslope measurements were taken as flow directions from striated pavements, flutes, grooves, tool marks, and fold noses, and paleocurrent measurements were taken as dip and dip direction on cross-laminations, cross-beds, and macroform foresets (Fig. 4). A total of 57 measurements (12 in the Guandacol Formation at Huaco and 45 in the Malanzán Formation at OMPV) were taken (Fig. 5). At OMPV, sections were measured in both segments of the paleovalley system to obtain a full understanding of upstream and downstream (proximal and distal) depositional environments.

4.2. Detrital zircon U–Pb geochronology analyses methods

This study makes use of previously published detrital zircon data for the strata in question, with one additional sample from the upper Guandacol Formation to allow for a full comparison of provenance through time during the glacial-to-post-glacial transition (Figs. 3 and 4). One sandstone sample (CDH0923-3 S) for detrital zircon analysis was collected from the AH locality. The sample was prepared according to methods laid out by Gehrels (2011) and U–Pb ages were determined for all zircons at the University of Arizona LaserChron laboratory (ALC). Zircons were extracted by traditional methods of crushing and grinding, and were separated using a Wilfley table, heavy liquids, and a Frantz magnetic separator to remove high-U zircons that could yield discordant results (Sircombe and Stern, 2002; McKay et al., 2018). The sample analyzed at ALC contained 75 zircons, which were hand-picked and mounted from a sieved 63–250 μm size-fraction. U–Pb geochronology of the zircons was conducted by laser ablation inductively coupled plasma mass spectrometry (LA-ICPMS). The sample was analyzed using a Thermo Element2 single-collector ICPMS. Data collected at the ALC were reduced using their Excel age calculation program (see Gehrels et al., 2008; Gehrels and Pecha, 2014). To eliminate results of analyses with common-Pb contamination or Pb loss, criteria for rejection included the following:

1 High errors (>10% uncertainty) of $^{206}Pb/^{207}Pb$ and $^{206}Pb/^{238}U$ isotope ratios
2 High ^{204}Pb values
3 Low $^{206}Pb/^{204}Pb$ ratios

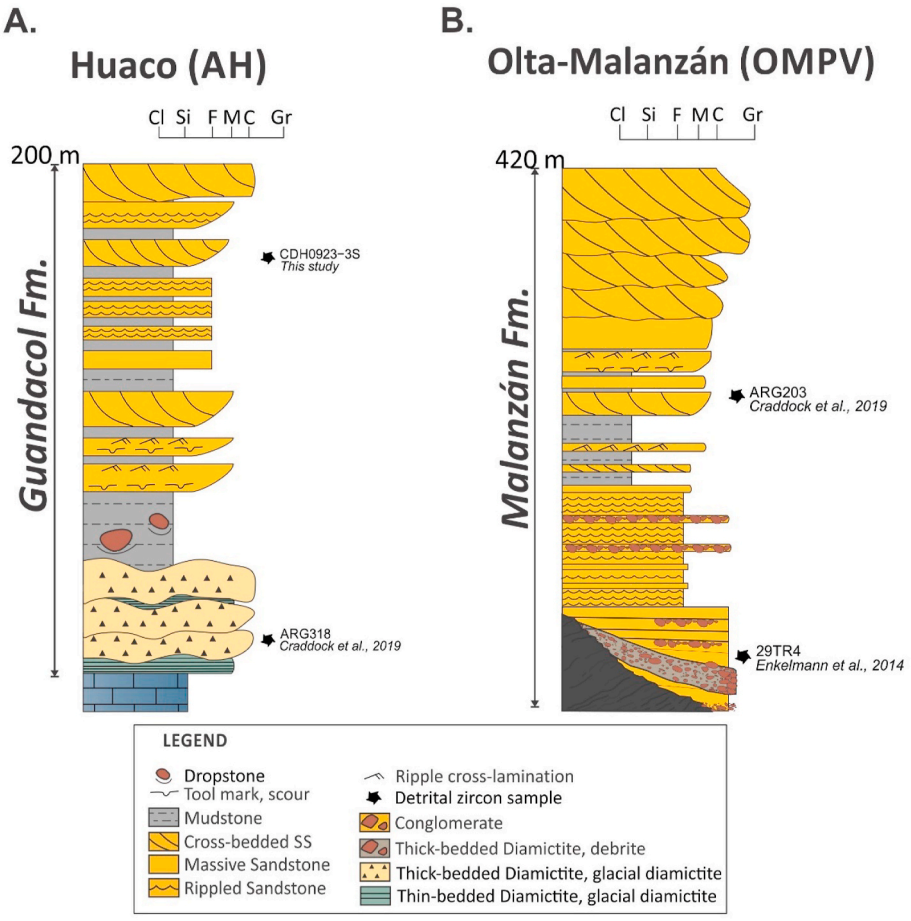

Fig. 4. Generalized and simplified stratigraphic columns displaying the facies and sedimentary structures identified in this study. Column A represents the facies of the Guandacol Formation found at the Agua Hedionda anticline at Huaco (AH). Column B represents the facies of the Malanzán Formation found within the Olta-Malanzán paleovalley system in the Sierras de Chepes and Los Llanos region.

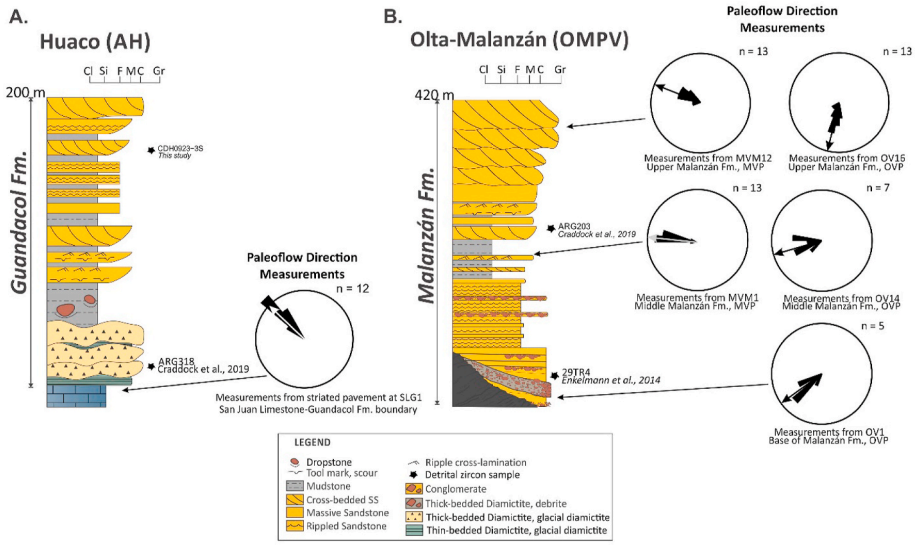

Fig. 5. Simplified stratigraphic columns for the Guandacol and Malanzán formations. Detrital zircon sample within the sections indicated by stars. Paleoflow orientations collected from strata (at OMPV only) or striated pavements (at Huaco only) depicted using rose diagrams with number of measurements (n). The paleoflow locations reference those mapped in Fig. 3.

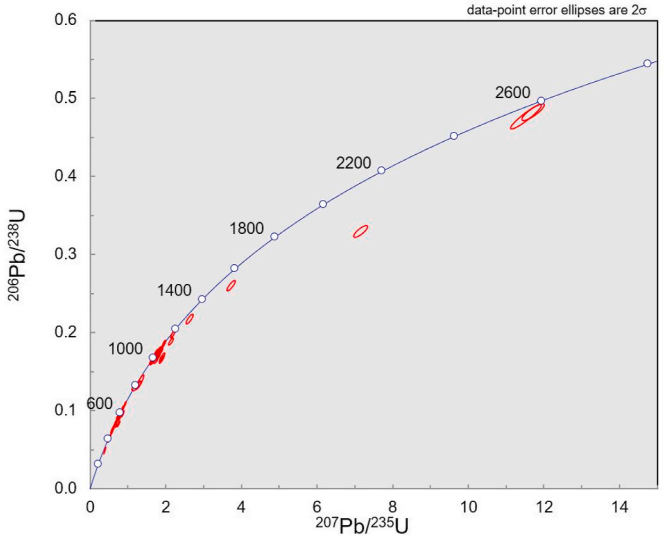

Fig. 6. Concordia plot of all analyzed concordant and discordant zircon U–Pb measurements for detrital zircon sample CDH0923-3 S from the Malanzán Formation, OMPV locality. See Fig. 3B for exact location.

4 High discordance (>20%) or reverse discordance (>5%)

The analyses that presented these criteria were removed from interpretations and are listed with the full list of analyses in Appendix A.

Once the data were obtained, all accepted analyses were used to create a Concordia diagram (Fig. 6) using Isoplot 4.15, a Microsoft Excel add-in from Ludwig (2012). The data here are discussed in the context of previously published ages from other strata of the Paganzo Group (cf. Enkelmann et al., 2014; Craddock et al., 2019). The data are also compared to published ages of igneous and metamorphic basement lithologies to determine provenance through time in the Paganzo Basin (e.g. Huff et al., 1998; Pankhurst et al., 1998; Rapela et al., 1998; Ottone et al., 2001; Dahlquist et al., 2010; Drobe et al., 2011; Verdecchia et al., 2011, 2014; 2018; Sial et al., 2013; Einhorn et al., 2015; Rapela et al., 2018).

Three out of the four samples used here are previously published data. For the Guandacol Formation, the oldest-strata (i.e. lowermost) sample was previously reported in Craddock et al. (2019; ARG318) from a glacigenic diamictite above the contact with the San Juan Limestone (Fig. 4A). The second post-glacial Guandacol sample is newly presented here (CDH0923-3 S) and is from a wavy-bedded sandstone in the uppermost Guandacol Formation. The two Malanzán Formation samples (i.e. lowermost and middle) used for reference in this contribution are previously reported (Fig. 4B). The first Malanzán Formation sample is from a study conducted by Enkelmann et al. (2014; 29TR4) and comes from a sandstone at the base of the formation near section OV1 (Fig. 4B) described in Moxness et al. (2018). The second Malanzán Formation sample is from a compilation published by Craddock et al. (2019) and is sampled from the middle part of the formation, in a thick succession of interbedded mudrock and sandstone beds. The samples from Craddock et al. (2019; ARG318 and ARG203) were also analyzed at ALC using the same criteria and methods. The sandstone sample used for reference for the lowermost Malanzán Formation comes from Enkelmann et al. (2014; 29TR4), and was analyzed using LA-ICP-MS (at the Museum für Mineralogie und Geologie in Germany) according to the methods described in Enkelmann et al. (2014), and the raw data can be found in the Geological Society of America Data Repository (item 2014126). For a more robust analysis of the entire region, more detrital zircon geochronology data are warranted, but were outside the scope of this study.

5. Lithofacies analysis

Outcrops of the Paganzo Group strata are exposed at the surface along both the western and eastern margins of the Paganzo Basin. At Olta-Malanzán, the base of the Malanzán Formation overlies basement, but is only exposed at the surface in the easternmost (i.e. towards Olta; OPV) portion of the paleovalley system (Fig. 3). The Malanzán Formation was measured at several locations throughout both the eastern and western (i.e. towards Malanzán; MPV) ends to get a full picture of the changes in depositional environments. At the base, the Malanzán Formation is dominated by sandstones and conglomerates (depending on location in the paleovalley) that directly overlie basement material without any grooves or striations to indicate glacial activity. The middle units of the formation at both ends of the paleovalley system record either an abrupt or an overall fining upward trend, indicating a local flooding event (Fig. 4). The upper members of the Malanzán Formation

record a coarsening-upward and a progradational setting as indicated by a transition from interbedded mudstone and sandstones to sandy clinoforms and conglomerates or conglomeratic sandstones (Fig. 4).

At Huaco, the base of the Guandacol Formation is exposed along the core of the anticline and is accessible in several locations south of Route 49 (formerly Route 40; Fig. 3B). The Guandacol Formation was measured at several locations along the eastern and western limbs of the anticline (Fig. 3B). The base of the formation overlies the San Juan Formation, which is an Ordovician limestone unit that comprises the core of the anticline. There are a few exposed striated pavements directly underlying the basal beds of the Guandacol Formation along this eastern limb and that were used to determine paleoflow direction (Fig. 5A). The base of the Guandacol Formation is dominated by thick- and thin-bedded and massive diamictites that tend to interfinger with each other indicating changes in proximal and more distal depositional settings. The diamictites transition into sandstones and mudstones that comprise a fining upward trend which culminates in a black shale. Above the black shale, interbedded sandstone and mudstones dominate the formation and contain evidence of soft sediment deformation and grooves. The top of the Guandacol Formation contains a coarsening-upward succession with the introduction of sandstones near the boundary with the overlying Tupe Formation.

5.1. Facies 1 – diamictite facies

5.1.1. Description

The diamictite facies is found at each of the sections and can be divided into two distinguishing groups: thick-bedded diamictites and thin-bedded diamictites. The clast-rich thick-bedded diamictite subfacies at OMPV overlies the sandstone facies near the contact with basement material (OV1 of Moxness et al., 2018, Fig. 7A). This diamictite is primarily a sandy diamictite, and it is massive with little to no internal structures, but in some areas inverse grading is noted and contains boulders that protrude into the overlying facies. Additionally, some wedge-shaped bodies are present, but are otherwise tabular in shape; this subfacies contains beds up to 1 m thick. The grains and clasts are angular to subrounded clast shapes, and range in size from coarse sand, and granules to cobbles, as well as boulders. All grains and clasts are granitic or granodiorite and metamorphic (schist or phyllite) in lithology. No striated clasts were observed. The contacts are sharp with boulders and cobbles protruding into overlying sandstone, while lateral boundaries either wedge out or end in an overhanging boulder nose with

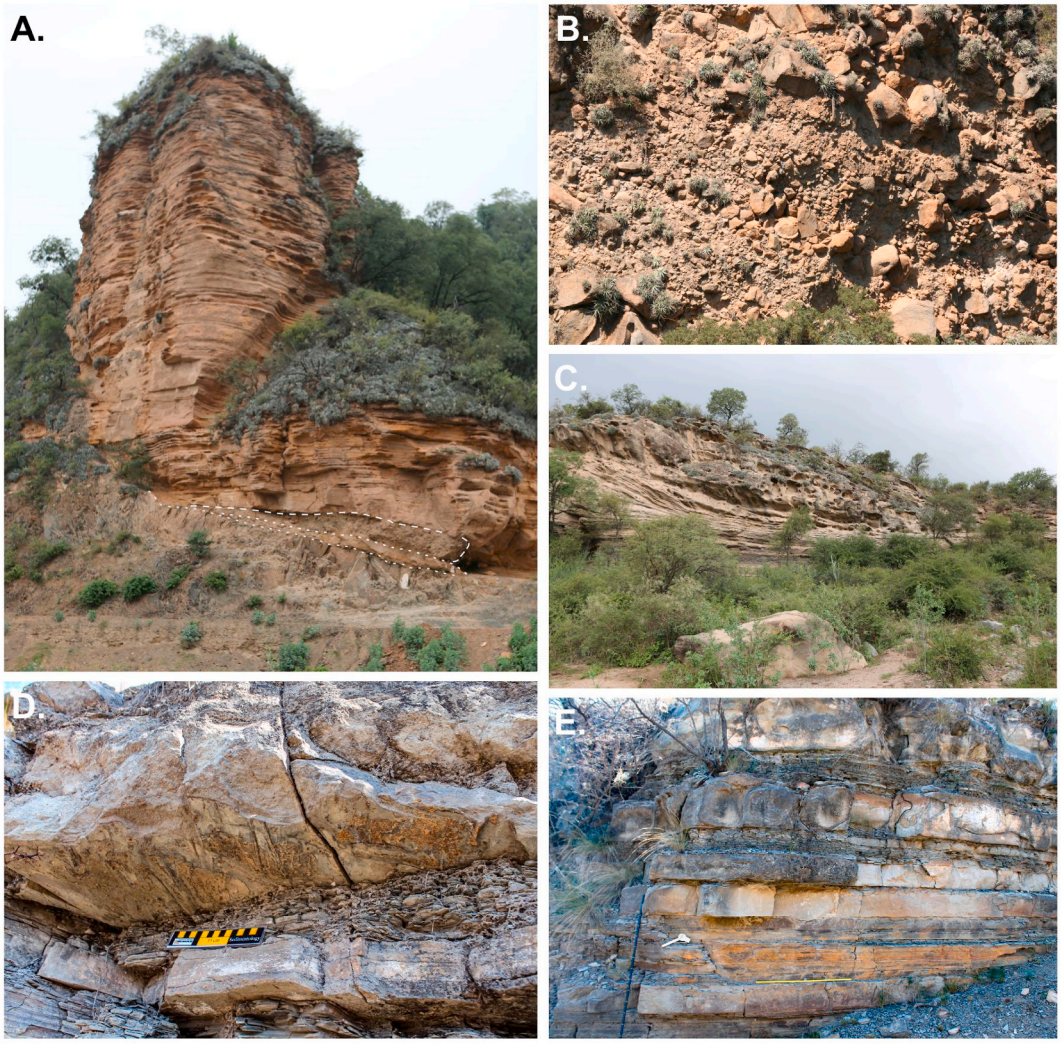

Fig. 7. Exposures of the Malanzán Formation at OMPV. A. Base of Malanzán Formation at OMPV locality. The diamictite facies (debris flow within the white dashed lines) overlying sandstone facies and basement (Olta phyllite and schist). Location of sample 29TR4 from Enkelmann et al. (2014). B. Conglomerate facies from a tributary paleovalley. Note dip of clinoforms to the right. C. Gilbert delta with a S-SW paleocurrent measurement from the upper Malanzán Formation, OPV. Note the occurrence of topset, foreset and bottomset beds. D. Tool marks from interbedded mudstone and sandstone facies in the MPV: MVM1 locality near the location of sample ARG203 from Craddock et al. (2019). E. Interbedded mudstone and sandstone facies in the MPV.

graded, granule to coarse-grained sandstone beds onlapping onto the nose.

At Huaco, the clast-rich to clast-poor, matrix-supported thin-bedded diamictite overlies the basement rock, the San Juan Limestone. This subfacies consists of coarse-grained clast sizes (granules to cobbles with rare boulders) within a silt-sand matrix (Fig. 8B and C). The clasts are primarily limestone with rare granitic and metamorphic lithologies, and most displayed either facets or striations and are on occasion bullet-shaped. Sub-decimeter scale marl beds are infrequently interbedded within the stratified diamictite units. The thin-bedded units are approximately 1 m thick and are cut into by a sandstone facies that vertically fines into interbedded mudstones and sandstones. Above this is a transition into 2–3 m of thick-bedded and more massive diamictite units that become more clast-supported than matrix-supported upward (Fig. 8D). The clast lithologies do alternate in dominance between the two subfacies (i.e. carbonate rocks dominate the diamictite facies, and granitic and metamorphic lithologies in other facies), but clast size on average seems to increase with smaller boulder and cobbles becoming more frequent upward in the section.

5.1.2. Interpretation

Diamictites are generated by numerous processes and do not always indicate the presence of glaciers (Lawson, 1979; Visser, 1983; Ashley et al., 1985; Powell and Domack, 2002; Eyles and Eyles, 2010; Vesely et al., 2018; Dietrich et al., 2019). In this study we present two diamictite facies that are genetically different. To determine the exact depositional processes, and therefore the depositional environment, a list of criteria was noted for each of the two localities: diamictite characteristics (thickness, class size trends, support mechanisms, presence/absence of internal shear planes, deformational structures etc.), the shape of outsized clasts, the presence or absence of striations on clasts, the presence of grooves and striae (i.e. iceberg keel marks or striated/grooved pavements) on underlying facies or basement material, and clast lithology. Using these features as a guide, a glacial/nonglacial environment can be inferred.

The clasts within this subfacies are often subrounded to angular and are poorly sorted, and in some instances are inversely graded within the diamictite bodies, but none were striated. Furthermore, the wedge-shaped bodies have preserved flow noses as well as boulders protruding from the tops of the deposits, indicating they are debris flows. The lack of any striated, bulleted or faceted clasts, the overwhelming dominance of local clast lithologies, as well as the complete lack of any striated pavements indicates that the debris flows are not resedimented glacial diamictites. Instead, the Olta-Malanzán paleovalley is housed within narrow, steep valley walls, which presents the ideal conditions for debris flows off the valley walls and into standing bodies of water within the central axis of the paleovalley (cf. Van Steijn, 1996; Godt and Coe, 2007). Based on studies of other debris flow characteristics, the thick-bedded sandy diamictite at OMPV is interpreted as a mass transport deposit, specifically as subaqueous debris flows (cf. Potsma et al., 1988; Mulder and Alexander, 2001; Sohn, 2000; Talling et al., 2012; Moxness et al., 2018, Fig. 7A).

At Huaco, the thin-bedded diamictites are also interpreted as mass transport deposits, but in this case, these debris flows are resedimented deposits in distal glaciomarine depositional settings (Fig. 8B and C). There are numerous lines of evidence to support this interpretation. The outsized clasts in this subfacies are striated, and some are bullet-shaped and faceted. The clast lithologies were predominantly local (i.e. carbonate), and to a lesser degree granitic and metamorphic, which are considered to be exotic as these lithologies do not occur within this area of the Precordilleran terrane (Keller, 1999; Marenssi et al., 2005). Furthermore, directly underlying this subfacies are numerous striated and grooved pavements on the San Juan Limestone, which serves as the basement for this locality.

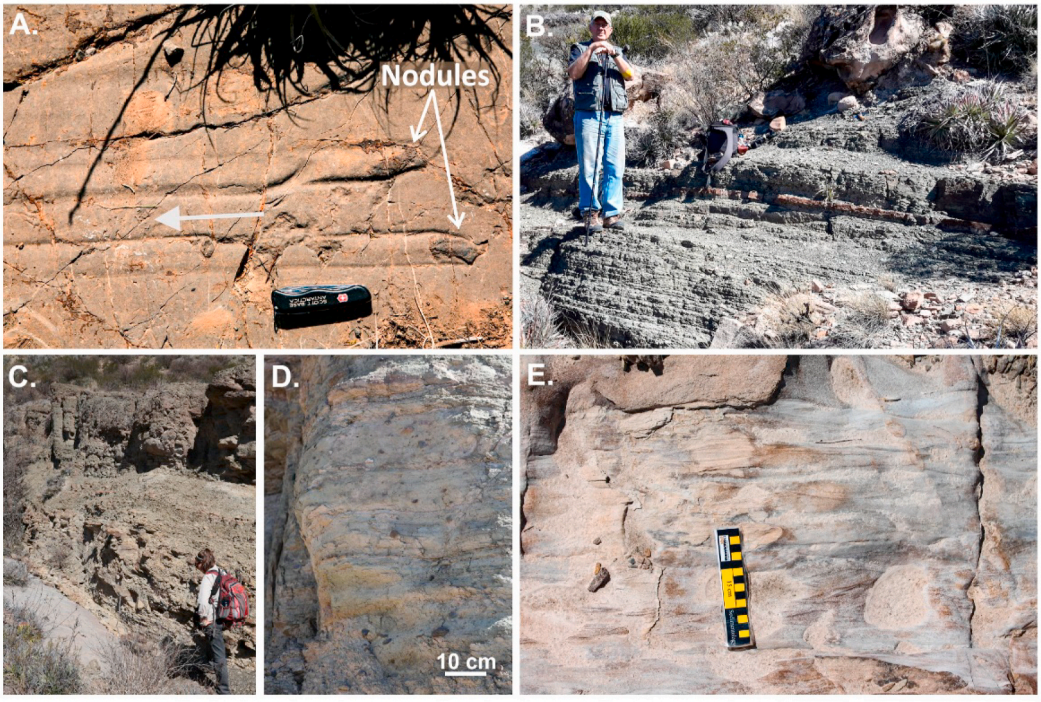

Fig. 8. Exposures of the Guandacol Formation and its contact with the San Juan Limestone at Huaco. A. Glacial grooves around siliceous nodules in San Juan Limestone (AH). Arrow indicates ice flow direction. B. Thin-bedded diamictite facies 4 m above the contact with the San Juan Limestone with a marl bed. C. Thin-bedded diamictite facies directly overlying San Juan Limestone. D. Thick-bedded diamictite facies. E. Wavy bedding within the uppermost Guandacol Formation, near the location of sample CDH0923-3 S.

5.2. Facies 2 – conglomerate facies

5.2.1. Description

The conglomerate facies is found only at OMPV and comprises a large portion of the lower member of the Malanzán Formation in areas where tributary paleovalleys join the main paleovalley (Fig. 7B). The base of this facies is erosional and overlies various other facies. This facies often cuts into finer-grained facies and laterally interfingers with finer-grained facies towards and down the axis of the paleovalley. The sandy matrix in the lower part of this facies gives way to thick bedded, cobble and boulder-supported conglomerates in the upper portion. The beds themselves are on average internally massive, but some beds display normal grading while others display inverse grading (Fig. 7B). Downlapping onto other facies is abundant, and undeformed beds display inclinations, or depositional dips (Fig. 7B). Some of the packages within this facies are wedge shaped, and decrease in thickness (i.e. pinch out) towards the paleovalley axis going from several meters to 1 m or less in thickness over a distance of tens to a hundred meters along exposures. All clast and boulder lithologies are dominated by granitic or granodiorite (i.e. Chepes granodiorite, Tuaní granite) and schist and phyllite cobbles (i.e. Olta metamorphic complex). Laterally and vertically, these conglomerates interstratify with sandstone facies and laminated mudstone facies. Internally these conglomerates cut down into underlying sediment packages, especially where they meet the valley walls. Towards the central axis of the paleovalley system, these conglomerates normally grade into finer-grained facies (i.e. sandstone facies and interbedded mudstone and sandstone facies).

5.2.2. Interpretation

The conglomerate facies in the Olta paleovalley is thoroughly described and discussed in Moxness et al. (2018). Since this facies downlaps, interfingers with, and grades laterally into finer-grained facies, and also contains boulder conglomerate clinoforms, the overall facies is interpreted as fan deltas, or where they may be subaerially exposed, alluvial fans. As such, these conglomerate bodies are the result of deposition in a high-energy environment subjected to numerous sediment gravity flows and rock falls from valley walls and tributary paleovalleys. These deposits then transition to sheet floods, non-cohesive and cohesive sediment gravity flows (i.e. coarse-grained debris flows) that are associated with high discharge events in a multi-channel fan delta system. The conglomerate facies is also found in the Malanzán paleovalley, but to a lesser degree.

5.3. Facies 3 – laminated mudstone facies

5.3.1. Description

The base of this facies at both localities is gradational with underlying interbedded mudstone and sandstone facies. At the OMPV, this facies consists of silt and clay-sized particles and is punctuated occasionally by fine to very-fine grained sandstone beds that pinch out laterally into the mudstone. At Huaco, this facies is silt and clay at the base and fines into a black shale at the top. Throughout the OMPV system, the mudstone facies contains frequent impressions of plant fossils (i.e. *cordaites sp.*), and in some sections contains hummocky cross-laminated, very fine-grained sandstones. At Huaco, the base of this facies drapes over the ripples that occur where this facies overlies the interbedded mudstone and sandstone facies, but is otherwise dominated by centimeter-scale laminations throughout without any other discernible internal structures. In the OPV, the mudstones are continuous, several meters thick, and rarely interrupted by granule to boulder outsized clasts of granodiorite and schist lithologies in areas proximal to the valley walls. In the MPV, this facies occurs in meter to sub-meter scale packages that are punctuated by units 3–10 cm thick of massive sandstone bodies. The upper boundary of this facies at both localities interfingers with the sandstone facies as well as the interbedded mudstone and sandstone facies above. Towards the upper part of the section measured in the MPV, this facies is also associated with centimeter-decimeter scale marl beds.

5.3.2. Interpretation

The mudstone facies at both localities represents a transition to a lower energy environment and deposition in an overall deeper water setting, below normal wave base. Both sections record flooding events. At Huaco, this has been interpreted to be a marine transgression (i.e. a late Mississippian-Early Pennsylvanian transgressive episode of Limarino et al., 2002a, 2006), and the mudstone facies at OMPV may be correlated to a regional rise in base level due to a potential marine transgression across the basin. It may also be due to the damming of the paleovalley by rock falls or by progradation of an alluvial fan across the valley. A marine interpretation of these deposits at OMPV has been supported by the presence of acritarchs within the middle member of the Malanzán Formation, and an interpretation of brackish marine conditions (cf. Gutiérrez and Limarino, 2001). The mudstone facies at OMPV contains some outsized clasts, which are interpreted here as either a product of falling detritus from the paleovalley walls, or rafting from surface ice formation (cf. Andreis and Bossi, 1981; Powell, 1984; Thomas and Connell, 1985; Gilbert, 1990; Bennet et al., 1994; Kempema et al., 2001; Powell and Domack, 2002). Several processes can transport clasts in inundated narrow valleys such as rock fall, the seasonal formation of lake or sea ice with an accumulation of clasts from mass-wasting and other alluvial processes, or by clasts trapped in root systems of floating plants. Some sections containing these outsized clasts were located near valley walls, and were composed of local, exposed bedrock, so we interpret the transport mechanism to be either surface ice formation, or rock falls. The loss of outsized clasts through the vertical succession is interpreted here as a cessation in either/or tectonic activity, or a change in climatic conditions that did not allow for the formation of surface ice. The mudstone facies associated with the sandstone stringers are most likely the result of distal hyperpycnal flows from periodic fluvial discharge events or from underflows potentially corresponding to storm activity where rare hummocky cross-stratification is noted within cm-scale sandstone horizons (cf. Lambert and Giovanoli, 1988; Martinsen, 1990; Bhattacharya, 2006; Crookshanks and Gilbert, 2008).

5.4. Facies 4 – interbedded mudstone and sandstone

5.4.1. Description

This facies is found at both localities, with some notable differences. Additionally, the interbedded mudstone and sandstone facies most often display sheet geometries, and less often as discontinuous bodies that had erosional to sharp bases at both localities. At OMPV, this facies is often comprised of 2–5 m-thick exposures of fine or medium-grained sandstones that grade into mudstones (i.e. high percentages of silt and clay, and at times with a very small percentage of lower very-fine grained sand size fraction; Fig. 7D and E). The centimeter to decimeter-scale medium-grained sandstone bodies are mostly internally-massive, but often also display sole marks along base of these packages and cross-laminations along the upper boundaries. At Huaco, the massive sandstone beds range in thickness from 10 to 25 cm. At both localities, the beds often contain medium-grained sand. Both in the Malanzán and Guandacol formations, some beds contain groove and prod marks as well as other soft sediment deformation at their base but internally, the beds are massive. At Huaco, these beds tend to be stacked vertically within 1-m thick packages and may display faint laminations just above the flute and grooves at the base. However, in some cases within the Malanzán Formation, these beds can occur as isolated folded and deformed pods within a finer-grained (very fine-grained sandstone to mudstone) matrix and are associated laterally with deformed units. Additionally, the facies at Huaco displayed grain-size differences that were less pronounced, with fine sand layers interspersed with silt-to very-fine sand interbeds. In the MPV, there are several levels of

grooves, tool marks (i.e. prod marks), and flutes (Fig. 7D). Rare gutter casts were also noted. These disappear up-section. One level of intense deformation within this facies was recorded. In areas proximal to the valley walls in the OPV, infrequent outsized clasts become rare and are finally lost altogether as the facies grades upward into the laminated mudstone facies at section OV14 in Moxness et al. (2018). At OMPV the dominant clast lithology was granitic/granodiorite within this facies, followed by schist and phyllite, all of which are local bedrock lithologies. In contrast, extremely rare to no outsized clasts were recorded within this facies at Huaco. At both localities, the facies grades normally into overlying facies or is cut into by overlying facies.

5.4.2. Interpretation

The presence of the thin planar and interbedded mudstone and sandstone facies association at both localities indicates a rapid and fluctuating change in environmental and depositional energy that is interpreted as gravity-driven deposits and rhythmites, more specifically turbidites (Talling et al., 2012; Talling, 2014). The appearance of horizontally laminated and massively-bedded sandstone bodies is consistent with the definition of the TD turbidite interval as described by Talling et al. (2012). The massive sandstone facies is found in both localities and records intervals of high-density flow deposition (Talling et al., 2012; Talling, 2014). Horizontally laminated sandstones are also deposited by geostrophic currents that represent return flow of water along the sea bottom away from coastlines during storm surges. Such events result in deep water deposition from episodic underflow currents (Basilici et al., 2012). The fine-grained horizontally laminated sandstone beds were most likely deposited by turbidity currents, hyperpycnal flows, or possibly underflows, and could have been triggered by slope failure or storm activity (cf. López Gamundí, 1997; Gani, 2004; Winsemann et al., 2007; Talling et al., 2012; Talling, 2014). The erosional lower contacts of the sandstones are likely due to scouring caused by turbulent currents (cf. Powell and Cowan, 1986; Boulton, 1990; Powell and Domack, 2002). The flutes and grooves found at the base of this facies represent current scour and scour by tools carried at the base of the flow in a distal deltaic environment. The deformed level at MPV displayed fold noses and axes that imparted a down-valley transport direction is interpreted as a down-slope mass transport deposit, and as there was internal deformation, it is classified as a slump (Talling et al., 2012; Talling, 2014). The association of deformed sandstones and mudstones within this facies indicates mass movements and sediment-gravity deposits from downslope movement of material off the valley walls, introduction by hyperpycnal flow off of the Gilbert Deltas, or storm-generated bottom currents down the paleovalley axis.

5.5. Facies 5 – cross-bedded sandstone facies

5.5.1. Description

The cross-bedded sandstone facies is found at both localities. The base of the cross-bedded sandstone facies at several sections is erosional, and cuts into multiple underlying facies, such as the interbedded mudstone and sandstone facies and the rippled sandstone facies. At OMPV this facies is noted at both ends of the paleovalley system within the middle member and also comprises most of the uppermost member of the Malanzán Formation. In the middle member of the MPV, the facies occurs in small, 0.5-m or less medium-grained sand size lenticular bodies within other facies, such as the interbedded mudstone and sandstone facies. In the uppermost member, the facies is found in gently to steeply-dipping clinoform bodies and foresets that fine and extend across outcrops as bottomset beds (Fig. 7C). Individual foresets can be traced into the underlying bottomsets in a down-valley direction. The facies in the OMPV is found in the middle member of the Malanzán Formation, where tributary valleys enter into the main paleovalley, and in a narrow portion of the main valley axis just before the valley increases in width. The facies is also present in the upper member of the Malanzán Formation throughout the paleovalley. At both ends of the paleovalley, the clinoforms are coarse-grained, and can range in grain size from granular and pebbly to conglomeratic. At Huaco, the facies is represented by medium-to-coarse-grained sandstone crossbeds within 0.5-m stacked bodies with erosional upper and lower boundaries. The sandstone facies cuts down into the symmetrically rippled sandstone facies (see section 5.6. below).

5.5.2. Interpretation

The cross-bedded sandstone facies represents periods of prograding or aggrading deltaic environments at both localities. In the lower and middle members of the Malanzán Formation (i.e. at both the Olta and Malanzán ends of the paleovalley), intervals of stacked cross-bedded sandstone bodies indicate deltaic systems building out into bodies of water most likely created by damming from the conglomeratic facies (cf. Moxness et al., 2018). They might also indicate progradation into a brackish marine embayment (cf. Gutierrez and Limarino, 2001; Buatois et al., 2010). Toward the top of the Guandacol Formation at Huaco, the cross-bedded facies overlies a symmetrically rippled sandstone, which indicates the progradation of deltaic systems into the area, and indicates a transition to more continental depositional processes, as this facies is erosionally overlain by fluvial sandstones of the Tupe Formation (Limarino et al., 2002b; Marenssi et al., 2005). The uppermost Malanzán Formation is preserved at both ends of the OMPV and contains this facies in 10+ meters-long sandy clinoforms that have both their topsets and bottomsets preserved. These sandstones represent prograding Gilbert-type deltas of high-gradient stream systems that are flowing into cold, dense waters of a proximal lacustrine or marine environment within the paleovalley system producing laterally extensive hyperpycnal (underflows) flows (cf. Stanley and Surdam, 1978; Colella et al., 1987; Nemec, 1990; Winsemann et al., 2007; Moxness et al., 2018). The preservation of extensive bottomset beds indicates that incoming waters continued away from the delta front as turbulent underflows.

5.6. Facies 6 – rippled sandstone

5.6.1. Description

The rippled sandstone facies can be found at both localities and can be broken down into two subfacies groups. Here we present symmetrically rippled subfacies, and asymmetrically-rippled sandstone facies. At Huaco, the two subfacies are found toward the upper portion of the formation. The base of the symmetrically rippled sandstone subfacies is erosional into the underlying asymmetrically rippled sandstone facies (Fig. 8E). On average, the ripples have a ripple index (RI) of 1 and are considered symmetrical, but in some cases are slightly asymmetrical. At OMPV, successions of symmetrically rippled sandstones are found to alternate with and gradationally overlie successions of asymmetrically-rippled sandstones. The asymmetrically rippled sandstone subfacies is present in both ends of the paleovalley and occurs in upper fine to medium-grained sand deposits. In some sections, this subfacies occurs gradationally above the massive sandstone facies, where in other locations it occurs gradationally above and below the symmetrically-rippled sandstone subfacies. In all sections, these ripples are often overlain by silt, or very-fine sand drapes.

5.6.2. Interpretation

The rippled sandstone subfacies is present at both localities and represents modification of sands by both wave and current activity. At Huaco, the symmetrical wave ripples are part of a coarsening- and shallowing-upward succession near the top of the Guandacol formation, indicating a progradation of a deltaic environment (cf. Schatz et al., 2011). At OMPV, the symmetrically-rippled sandstones suggest the reworking of a unidirectional flow deposit, or a bi-directional flow from wave activity (Baird, 1962; Reineck and Singh, 1980; Moxness et al., 2018). As indicated by Moxness et al. (2018), numerous levels of wave-rippled sandstones are found throughout the Olta paleovalley. However, the Malanzán end of the paleovalley is instead dominated by

asymmetrical ripples and are the result of unidirectional flow associated with turbidity or hyperpycnal currents.

6. Paleoflow and depositional environments

6.1. Paleoflow

The base of the Guandacol Formation at all Huaco localities contains subglacial and ice-proximal deposits and features (Marenssi et al., 2005; Limarino et al., 2014; this study). There, the Guandacol Formation has been measured and described in multiple studies (cf. López-Gamundí and Martínez, 2000; Limarino et al., 2002, 2005; Pazos, 2002; Marenssi et al., 2005; Henry et al., 2008; this study). Our observations of this section do not dispute previous findings, and the measured sections contain ample evidence of glacial processes, from striated pavements along the Cambrian-Ordovician San Juan Limestone, to stratified diamictites with striated and faceted clasts at the base of the section (Fig. 5). The paleoflow measurements are from a glaciated and striated pavement that exists on the upper surface of the San Juan Limestone (Fig. 5). The striations allow for interpretation of true glacial flow as there were grooves with plucking around siliceous nodules in the San Juan Limestone (Fig. 8A). The paleoflow of the glacier at Huaco was to the NW (i.e. 310-320°, with a vector mean direction of 313°; Fig. 5).

6.2. Depositional environment interpretations

The overall depositional environments interpreted from our analyses are consistent with previous studies. The glacial deposits of the lower Guandacol Formation at AH are overlain by thick successions of shales, interspersed with sandstones. The shales and sandstones are interpreted here as a local post-glacial transgression (i.e. a change in relative sea-level; Powell and Cooper, 2002) by multiple studies (Limarino et al., 2002, 2005, 2014). The shales are overlain by increasingly thicker packages of wavy-bedded sandstones and by planar laminated sandstones (Fig. 4). The depositional environment interpretation for the upper Guandacol Formation at Huaco is a progradational succession from offshore, to offshore-transition and then deltaic packages at the uppermost boundary with the overlying Tupe Formation.

The Malanzán Formation is the time-equivalent unit in the easternmost part of the Paganzo Basin occurs in the Olta-Malanzán paleovalley (cf. Bracaccini, 1948; Azcuy, 1975; Andreis et al., 1986;Azcuy et al., 1987 ; Buatois and Mángano, 1995; Sterren and Martínez, 1996; Net and Limarino, 1999; Net et al., 2002; Moxness et al., 2018; Pauls et al., 2019) and is correlated using the palynological assemblages (cf. Gutierrez and Limarino, 2001; Césari et al., 2011). These deposits have been reinterpreted as conglomerates, diamictites, sandstones and shales related to alluvial, fluvial, and lacustrine processes (Moxness et al., 2018; Pauls et al., 2019). The base of the section overlies basement material, Olta phyllite and schist, in an erosive manner and onlaps the Chepes granodiorite in some exposed locations (Fig. 7A; Moxness et al., 2018; Pauls et al., 2019; this study). No striated pavement, nor striations of any kind were recorded in the paleovalley where the Malanzán Formation overlies bedrock. Unlike glacial valleys, the OMPV narrows near tributary paleovalleys from several km wide down to less than 200 m wide. These tributary paleovalleys have coarse fan faces emanating from them indicating that they are of fluvial origin (Moxness et al., 2018). Additionally, the clasts present in the diamictite and conglomerate facies of the Malanzán Formation are not striated nor faceted, and paleocurrent measurements range from S-SW, parallel to the axis of the paleovalley throughout the Malanzán Formation (Figs. 3 and 5). While glacially-carved valleys are generally classified by their profile shape (i.e. U-shaped; MacGregor et al., 2000), the OMPV does not appear to display this geometry for the late Paleozoic sedimentary fill. The floor of the paleovalley narrows to less than 200 m across where paleotributary valleys appear to enter the main axis, which has not been recorded in glacial erosion models, nor in more recent glacially-excavated valleys (Montgomery, 2000; MacGregor et al., 2002; Anderson et al., 2006). Moxness et al. (2018) concluded that with the lack of glacial evidence and the geometry of the paleovalley at this location, the paleovalley could not have been carved by a glacier, or by glacial processes.

7. Detrital zircon geochronology results

Based on the availability of previously published detrital zircon geochronology data (cf. Enkelmann et al., 2015; Craddock et al., 2019) for the two localities (i.e. Huaco [AH] and Olta-Malanzán [OMPV]) discussed here, only one new detrital zircon geochronology sample was analyzed for this study (CDH0923-3 S).

7.1. CDH0923-3 S, Guandacol Formation, Huaco Locality

One sandstone sample was collected from a wavy-bedded meter-thick sandstone package from within a shoreface succession in the uppermost Guandacol Formation (Fig. 4). This sample contained 75 concordant zircons ranging in age from 2616.4 ± 8.9 Ma to 381.4 ± 3.3 Ma (Fig. 9). One primary age peak ranges from 480 to 440 Ma (Ordovician), with a component from 500 to 600 Ma (Cambrian-late Neoproterozoic), and a secondary peak at 1160-960 Ma (Fig. 9). In this sample, 1% of the zircons analyzed were Carboniferous, 5% were Devonian, 3% were Silurian, 20% were Ordovician, 10% were Cambrian, 27% were Neoproterozoic, and 28% were Mesoproterozoic.

7.2. Previously published geochronology samples

ARG318, Lowermost Guandacol Formation, Huaco Locality (Craddock et al., 2019).

This sample was collected from a diamictite at the base of the Guandacol Formation, in which both massive and bedded diamictite with dropstones included, and is here interpreted to be from a proglacial glaciomarine environment (Fig. 9). This sample contained 36 concordant zircons that range in age from 2059 ± 7.5 to 385.2 ± 5.9 Ma. For this sample, 3% of the zircons were Devonian, 20% were Ordovician, 44% were Cambrian, 19% were Neoproterozoic, 8% were Mesoproterozoic, and 3% were Paleoproterozoic (Fig. 9).

29TR4, Lowermost Malanzán Formation, Olta-Malanzán Paleovalley (Enkelmann et al., 2014).

This sample was collected from a debris flow deposit at the base of the Malanzán Formation (Fig. 4). The sample contained 93 concordant detrital zircons with ages ranging from 2203 ± 36 Ma to 333 ± 4.5. For this sample, 3% of the analyzed zircons were Carboniferous, 12% were Devonian, 3% were Silurian, 24% were Ordovician, 29% were Cambrian, 19% were Neoproterozoic, 3% were Mesoproterozoic, and 7% were Paleoproterozoic (Fig. 9).

ARG203, Middle-Upper Malanzán Formation, Olta-Malanzán Paleovalley (Craddock et al., 2019).

This sample was collected from a sandstone within a succession of interbedded mudstones and sandstones that are interpreted to be a prograding and fluctuating delta front system (Fig. 4). The sample contained 50 zircons that range in age from 937.3 ± 26.1 Ma to 362.7 ± 8.6 Ma. For this sample, 8% of the zircons were Devonian, 2% were Silurian, 54% were Ordovician, 20% were Cambrian, and 16% were Neoproterozoic (Fig. 9).

8. Discussion

The wide variety of clast lithologies, such as carbonates, granites and metamorphic rocks, in both the glacial diamictites and post-glacial deposits of the Guandacol Formation at Huaco indicate a mixture of potential source areas (cf. Marenssi et al., 2005; this study). The detrital zircon age populations for the Guandacol Formation samples (ARG318, CDH0923-3 S) indicate a relatively local provenance, with a primary age peak showing an Ordovician age source (470-450 Ma), and a secondary

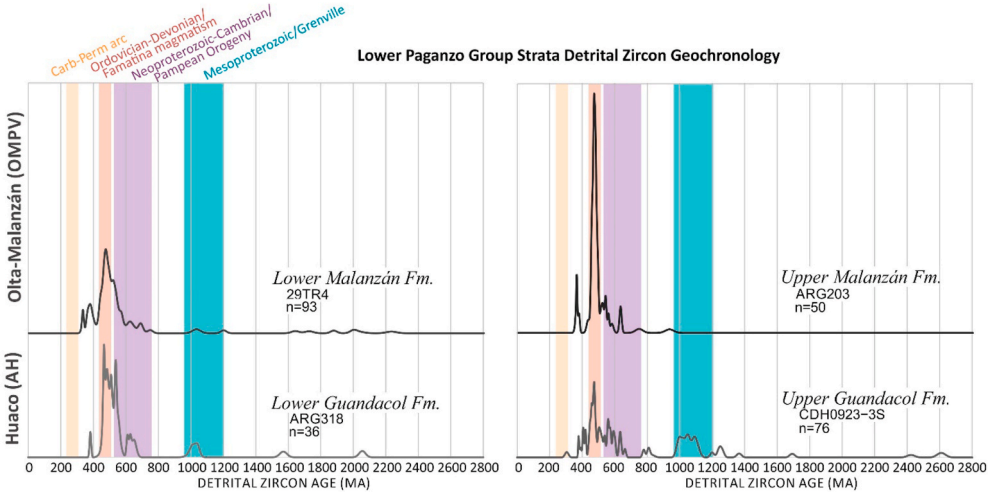

Fig. 9. Normalized probability distribution plots for the lower Paganzo Group strata. The samples are separated by localities: Huaco (AH) - Lower Guandacol Fm. – ARG318 (Craddock et al., 2019), Upper Guandacol Fm. – CDH0923-3 S (this study); Olta-Malanzán (OMPV) - Lower Malanzán Fm. – 29TR4 (Enkelmann et al., 2014), Upper Malanzán Fm. – ARG203 (Craddock et al., 2019).

peak with Mesoproterozoic ages (1200-900 Ma). Huaco is located within the Cuyania terrane, and just to the west of the westernmost Famatinian-aged granites in the Sierra de Valle Fértil, which contain crystallization ages within the range of the primary age peak for the detrital zircons of the Guandacol Formation (cf. Pankhurst et al., 2000; Dahlquist et al., 2010, Figs. 10 and 11). However, the glacial diamictites could also contain reworked sediments from the Ordovician and Cambrian sedimentary deposits of the Precordillera and Cuyania terranes (Huff et al., 1998; Ottone et al., 2001; Vujovich et al., 2004; Naipauer et al., 2010a; Sial et al., 2013, Figs. 10 and 11). Together, these early Paleozoic sources of the Precordilleran and Cuyania terranes provide the appropriate age range for the majority of the detrital zircons found in the Guandacol Formation at Huaco. The clast compositions found in the basal Guandacol sediments are consistent with these interpretations.

The older, less prominent peak of Mesoproterozoic ages can only be associated with basement material of that same age along the eastern margin of the Precordilleran and Cuyania terranes where there is known Mesoproterozoic basement, such as is found within the Sierra de Pie de Palo (Vujovich et al., 2004; Dahlquist et al., 2010; Naipauer et al., 2010a; Einhorn et al., 2015). Therefore, the Guandacol Formation at Huaco is likely derived from basement material similar in age to material from the Cuyania terrane and the westernmost edge of the Famatina magmatic belt (cf. Pankhurst et al., 2000; Vujovich et al., 2004; Dahlquist et al., 2010; Naipauer et al., 2010a; Einhorn et al., 2015), as these ranges contain material of both age sets. Furthermore, the NW paleoflow measurements from the striated and grooved surface cut on the San Juan Limestone discussed above also support this interpretation (cf. López-Gamundí and Martínez, 2000; Henry et al., 2008; this study; Fig. 5).

The upper Guandacol sample (CDH0923-3 S) is from the uppermost part the formation, after the post-glacial marine transgressive shales (Fig. 4). The sandstones here represent a wave-dominated deltaic environment, and there are no more striated clasts, nor outsized clasts recorded, and as such, any influence glacial ice had on the system is minimal to none. The detrital zircons, nonetheless, still indicate the same provenance signature, with a primary Ordovician peak and a secondary Mesoproterozoic peak (Fig. 10). Thus, the depositional system is still localized and reworking from the same system that sourced the glacial units.

The Olta-Malanzán samples also represent deposition during both glacial/cold-climate and post-glacial phases in the western Paganzo Basin, but indirectly, as there is no evidence of glaciation occurring in this paleovalley (Moxness et al., 2018; Pauls et al., 2019). The basement material that underlies this paleovalley contains late Cambrian to Ordovician metamorphic and granitoid rocks (Pankhurst et al., 1998, 2000; Dahlquist et al., 2010). The lowermost sample is from the base of the Malanzán Formation, and based on its primary age peak, reflects the early Ordovician Sierra de Chepes basement material (477–497 Ma; Pankhurst et al., 1998; Enkelmann et al., 2014, Figs. 10 and 11). The local lithology of the clasts (i.e. granodiorite, granite, schist, and phyllite) within the conglomerate and diamictite facies further supports this interpretation. The second Malanzán Formation sample is from the middle part of the formation, in a thick succession of interbedded mudrock and sandstone beds, which is correlated with the post-glacial transgression across the Paganzo Basin (Gutiérrez and Limarino, 2001). The detrital zircon age populations for both Malanzán samples are very similar and reflect ages found within the igneous and metamorphic provinces within the Sierra de Chepes and Los Llanos ranges (Fig. 10), and therefore represent a local provenance. The detrital zircon analyses have been interpreted by both Enkelmann et al. (2014) and Craddock et al. (2019) to represent local provenance, and the results from this study agree with their interpretations (Fig. 10). Furthermore, the samples are found along the main valley axis, with much of the depositional fill sourcing from the valley walls and tributary paleovalleys within the paleovalley system (Moxness et al., 2018).

Nevertheless, the fact that these two lower samples from the Guandacol and Malanzán formations have similar detrital zircon populations is not unexpected since most of the western margin of Argentine Gondwana is composed of metamorphic and igneous units of similar ages (Figs. 10 and 11; Huff et al., 1998; Pankhurst et al., 1998, 2000; Ramos et al., 1998, 2010, 2015; Rapela et al., 1998; Ottone et al., 2001; Sato et al., 2001, 2006; Vujovich et al., 2004; Rapalini, 2005; Dahlquist et al., 2010; Naipauer et al., 2010a, 2010b; Sial et al., 2013; Verdecchia et al., 2011, 2014; Einhorn et al., 2015). The main peaks for all four samples represent the sedimentary deposits following the Pampean orogeny (520–570 Ma; Pankhurst et al., 2000; Willner et al., 2008), as well as the Famatinian magmatic belt (500-440 Ma; Pankhurst et al., 2000; Enklemann et al., 2014), and sediments derived from those igneous bodies. A similar study conducted by Einhorn et al. (2015) looked at Neoproterozoic through Permian sedimentary deposits to the north of the Paganzo Basin, in Argentina and Bolivia. Comparing the results from this study to those of Einhorn et al. (2015), it is clear that all of the strata along the Panthalassan margin of Gondwana during this timeframe contains very similar detrital zircon populations (Figs. 10 and 11).

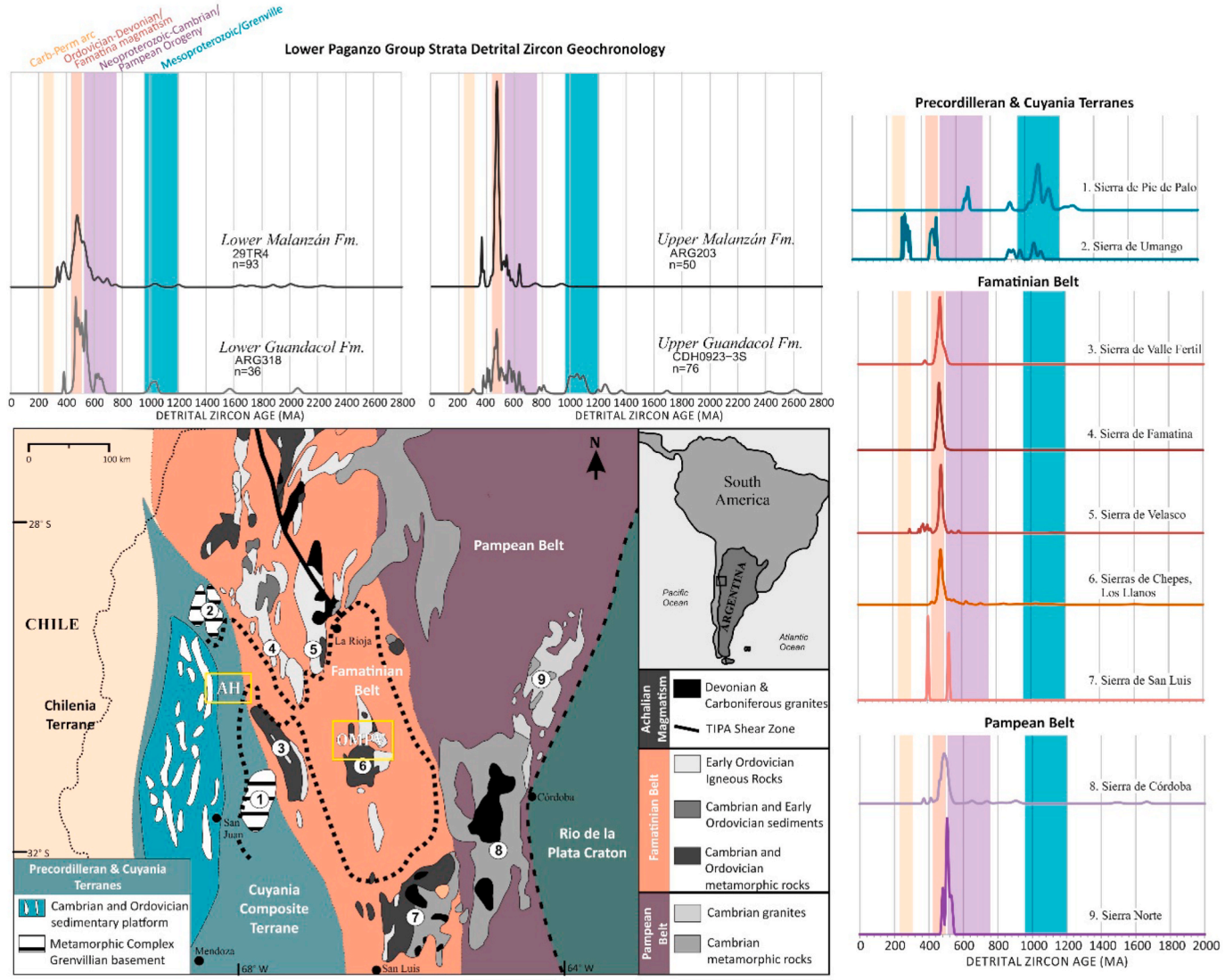

Fig. 10. Mesoproterozoic-Carboniferous igneous and metamorphic provinces for the Paganzo Basin area (demarcated by the dotted line) and their available zircon geochronology (n = 398). Map is modified from Dahlquist et al. (2010). The four samples considered in this study come from the two areas highlighted by the yellow boxes: AH, Lower Guandacol Fm. – ARG318 (Craddock et al., 2019), Upper Guandacol Fm. – CDH0923-3 S; OMPV, Lower Malanzán Fm. – 29TR4 (Enkelmann et al., 2014), Upper Malanzán Fm. – ARG203 (Craddock et al., 2019). Reference Fig. 3 for exact locations. The cited literature for the igneous and metamorphic zircon compilation is as follows: (1) Sierra de Pie de Palo - Vujovich et al. (2004); Naipauer et al. (2010a) (2) Sierra de Umango - Varela et al. (2003), 2005 (3) Sierra de Valle Fértil - Pankhurst et al. (2000) (4) Sierra de Famatina - Pankhurst et al. (2000) (5) Sierra de Velasco - Toselli et al. (2003); Pankhurst et al. (2000) (6) Sierras de Chepes, Los Llanos - Pankhurst et al. (2000) (7) Sierra de San Luis - Vujovich and Ostera (2003); Drobe et al. (2009) (8) Sierra de Córdoba - Rapela et al. (1998), Pankhurst et al. (2000) (9) Sierra Norte - Leal et al., 20003; Llambías et al. (2003). (For interpretation of the references to colour in this figure legend, the reader is referred to the Web version of this article.)

However, one stark difference between the two sample sets is the presence of early Carboniferous detrital zircons in the Malanzán Formation samples and the absence of these ages in the Guandacol Formation samples. This difference points to potentially separate depositional centers, as Devonian to Early Carboniferous intrusive post-orogenic granites are found throughout the central Famatina magmatic belt (cf. Dahlquist et al., 2010; Martina et al., 2018), which corresponds to the central portion of the Paganzo Basin. If there were an ice sheet that drained from the eastern Sierras Pampeanas, then detrital zircons of early Carboniferous ages would be expected at both localities. Detrital zircons of these ages are only present at OMPV and not at Huaco (Fig. 10), providing evidence that these two localities do not share a depositional connection.

Another major difference between the two Paganzo Basin sample sets is the lack of prominent peaks of Mesoproterozoic detrital zircons for the Malanzán Formation, where in contrast to both of the Guandacol Formation samples which contain strong detrital zircon Mesoproterozoic peaks (Fig. 11). In the Cuyania and Precordilleran terranes, many studies have found Mesoproterozoic crust underlying the Sierra de Pie de Palo, Sierra de Umango and Sierra de Maz, and is therefore interpreted to be a remnant of the Brasiliano-Pan-African belt (Vujovich et al., 2004; Dahlquist et al., 2010; Thomas et al., 2015; Rapela et al., 2018), or a part of Laurentia. We interpret these ranges to be the sources for the Mesoproterozoic zircon populations in the Guandacol Formation samples, but not the Malanzán Formation samples. Instead, the Mesoproterozoic zircons within the Malanzán Formation are most likely sourced and subsequently reworked from Mesoproterozoic-aged metamorphic rocks that have been mapped and identified to the east, south and north and of the Sierra de Chepes and Los Llanos ranges, in the Sierra de San Luis and Sierras de Córdoba (Sato et al., 2001, 2006; Drobe et al., 2009, 2011; Rapela et al., 2018). Mesoproterozoic ages are also found in older metasedimentary units, such as the Puncoviscana

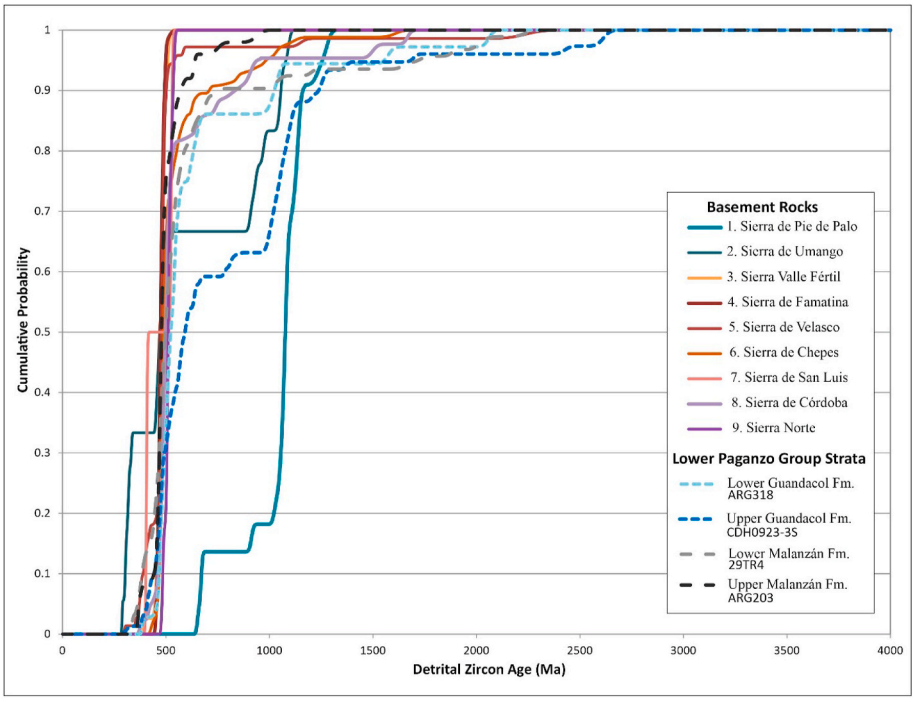

Fig. 11. Cumulative probability distribution for the four Paganzo Group samples and the basement units in the region. Lower Guandacol Fm. – ARG318 (Craddock et al., 2019), Upper Guandacol Fm. – CDH0923-3 S, Lower Malanzán Fm. – 29TR4 (Enkelmann et al., 2014), Upper Malanzán Fm. – ARG203 (Craddock et al., 2019). The cited literature for the igneous and metamorphic zircon compilation is as follows: (1) Sierra de Pie de Palo - Vujovich et al. (2004); Naipauer et al. (2010a) (2) Sierra de Umango - Varela et al. (2003), 2005 (3) Sierra de Valle Fértil - Pankhurst et al. (2000) (4) Sierra de Famatina - Pankhurst et al. (2000) (5) Sierra de Velasco - Toselli et al. (2003); Pankhurst et al. (2000) (6) Sierras de Chepes, Los Llanos - Pankhurst et al. (2000) (7) Sierra de San Luis - Vujovich and Ostera (2003); Drobe et al. (2009) (8) Sierra de Córdoba - Rapela et al. (1998), Pankhurst et al. (2000) (9) Sierra Norte - Leal et al., 20003; Llambías et al. (2003).

Formation further to the north in northern Argentina and Bolivia (Rapela et al., 2018). The paleocurrent data indicate (i.e. SW; Fig. 5) that the Sierra de San Luis and the Puncoviscana Formation would likely not have been a source for the Carboniferous strata. That is not to say that there could not be recycling of these grains from the Neoproterozoic-Cambrian metamorphic units in the Sierras de Chepes and Los Llanos, as well as to the east in the Sierras de Córdoba, which certainly could have supplied the limited number of grains that were measured in the lowermost sample.

9. Evidence for mid-Carboniferous ice extent in the Paganzo Basin

The Guandacol Formation at Huaco presents several lines of evidence for glacial presence in the western margin of the Paganzo Basin. First is the presence of the striated pavement along the uppermost surface of the San Juan Limestone, which serves as the contact with basement in this location of the Guandacol Formation (Fig. 4). The directions of the striae from that study (i.e. 300°-120°; Marenssi et al., 2005) are in agreement with the NW-SE directions we recorded on the eastern limb (ranging from 310°-320°; Fig. 5), and also aligns with descriptions from López Gamundí and Martínez (2000). The inferred flow direction of glacial ice at the base of the Guandacol Formation was in a NW (mean vector of 313°; Fig. 5) direction based on the measurements taken from grooves around eroded nodules on the limestone surface (Fig. 8A). Additionally, directly above the striated contact with the San Juan Limestone, several meters of thin and thick-bedded diamictite were measured and these strata contained numerous striated and faceted clasts, some with characteristic bullet shapes. With the occurrence of each of these lines of evidence, we can conclude that glacial ice was present in the vicinity of the Huaco locality during the Serpukhovian-Bashkirian glacial phase of the Paganzo Basin.

In contrast to the ample lines of glacial evidence in the lower Guandacol units at Huaco, as well as other localities along the western margin of the Paganzo Basin (cf. Scalabrini Ortiz, 1972; Andreis et al., 1975; López-Gamundí and Amos, 1985; Buatois and Mángano, 1994; López-Gamundí and Martínez, 2000; Kneller et al., 2004; Henry, 2007; Henry et al., 2008, 2010; Isbell et al., 2012; Aquino et al., 2014; Valdez-Buso et al., 2017, 2020; Limarino et al., 2014; Alonso-Muruaga et al., 2018), the Malanzán Formation does not display any evidence of glaciation within the basal and middle units (this study; Moxness et al., 2018; Pauls et al., 2019). There is a lack of any glacial evidence, such as faceted and/or striated clasts; there were no striae found on exposed basement lithologies, even where there was direct contact with the Malanzán Formation; and the diamictite morphology at the base of the Malanzán Formation is indicative of formation via debris flows in an alluvial fan and lacustrine environment rather than from morainal bank or pro-glacial depositional processes (cf. Andreis et al., 1986; Buatois and Mangano, 1995; Socha et al., 2014; Moxness et al., 2018). Paleocurrent measurements from the base of the Malanzán Formation indicate a more south-southwesterly direction (Fig. 5), which indicates flow within the confines of the paleovalley, and does not correspond to the paleoflow measurements in the western proto-Precordilleran domain of the Paganzo Basin.

When comparing the clast lithologies for the two localities, the sections record very different clast lithologies. For example, at Huaco, the Guandacol Formation contains clasts comprised of carbonates, high-grade metamorphic rocks, and granites. As noted in our descriptions, and also supported by Marenssi et al. (2005), the diamictite facies are dominated by carbonate clast lithologies, while the interbedded sand and mudstone facies are dominated by the high-grade metamorphic and granitic lithologies. The dominant lithology appears to correspond to changes in depositional settings, which is a reflection of the change in source materials and erosional patterns, and ultimately, provenance. In the literature, it is interpreted that the carbonate clasts of the glacial deposits represent local basement lithology within the Precordilleran terrane, such as the San Juan Limestone, and Los Azules and Talacasto formations (Huff et al., 1998; Ottone et al., 2001; Sial et al., 2013), while the other lithologies (i.e. the metamorphic and igneous clasts) in the ice-retreat facies are representative of more distal sources from the Sierras Pampeanas (cf. Marenssi et al., 2005). Once ice retreated from exposures of Cambrian-Ordovician limestones, there would no longer be a carbonate source. Icebergs, however, would transport clasts that the retreating glacier was eroding and transport them to the Agua Hedionda anticline area after calving and iceberg transit. The detrital zircon geochronology results of the lower Guandacol Formation samples

(ARG318; Craddock et al., 2019) further support the interpretation that the glacial deposits are likely sourced from more local basement lithologies found within, and possibly just beyond, the Cuyania terrane (Fig. 10). Cambrian ages are the dominant ages (44%), followed by Ordovician and Neoproterozoic ages (20 and 19% respectively; Fig. 12). These ages also correspond to findings from a U–Pb zircon geochronology study presented by Valdez Buso et al. (2020), where samples of the Guandacol Formation at other localities have similar Mesoproterozoic age populations (Figs. 10 and 11). We can therefore conclude that the sources for these grains are coming from local sources within the Cuyania and Precordilleran terrane regions, and not from further to the east in the Paganzo Basin, such as the eastern Sierras Pampeanas.

On the other side of the basin, the Malanzán Formation records a similar trend of provenance based upon the clast lithologies. The clasts in the lower Malanzán Formation are predominantly granodiorite with lesser amounts of schist and phyllite clasts. All three clast types can be traced to bedrock lithologies in the Sierras de Chepes (Pankhurst et al., 1998, 2000). The detrital zircon geochronology results further support this interpretation. The bedrock of this paleovalley system is Cambrian-Ordovician in age, and the age peaks from these samples are predominantly Cambrian and Ordovician (29% and 24% respectively in sample 29TR4; and 20%, 54% respectively in sample ARG203), followed by Neoproterozoic ages (19% in sample 29TR4, and 16% in sample ARG203). The Sierra de Chepes region is approximately 475–480 Ma, and therefore can account for the dominant ages in the samples (Pankhurst et al., 2000). The Neoproterozoic ages most likely come from the Olta schist and phyllite that is found within the Sierras de Chepes range, and could also potentially be sourced from rocks that are mapped further

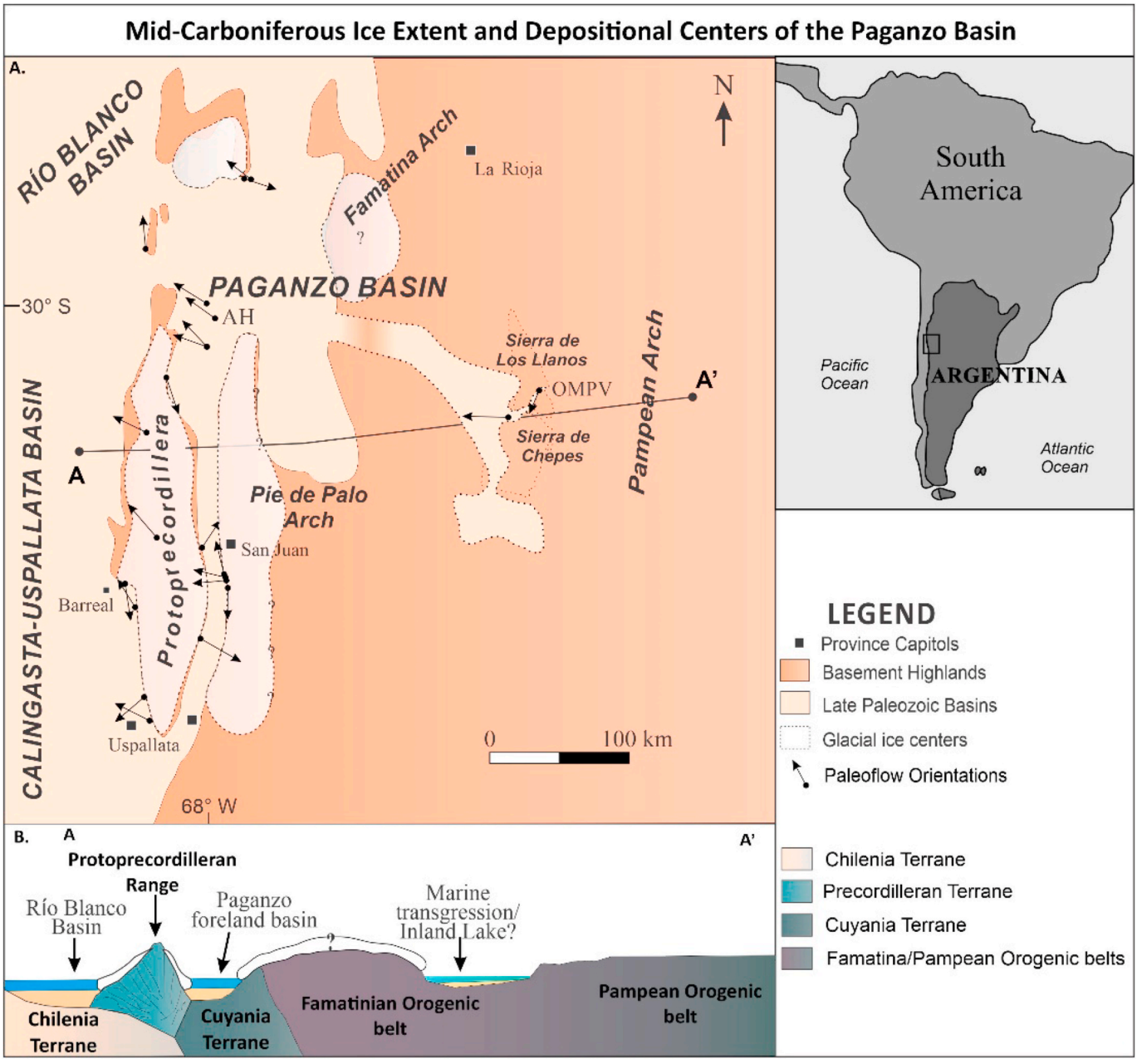

Fig. 12. The revised depositional environment and glacial extent model for the mid-Carboniferous Paganzo Basin. A. Ice centers and glacial deposition restricted to the western Paganzo Basin and Calingasta-Uspallata and Río Blanco basins. Paleoflow directions are from the same dataset as in Fig. 1. Basin reconstruction map modified from López Gamundí et al. (1994). Paleoflow directions modified from Henry et al. (2008) and Moxness et al. (2018). B. Cross-section of the western margin of Gondwana with ice centers highlighted. Tectonic cross-section modified from Henry et al. (2008) and Moxness et al. (2018).

to the east, such as those identified in the Sierras de Córdoba (Rapela et al., 1998; Leal et al., 2003; Llambías et al., 2003; Toselli et al., 2003). A few more prominent age populations occur in the Malanzán Formation samples that are not as prevalent or even present in the Guandacol Formation samples, and correspond to Silurian, and Devonian to early Carboniferous ages (Fig. 8). These ages likely correspond to early-middle Paleozoic post-orogenic granites that exist within and along the Famatina belt, and into the eastern Sierras Pampeanas, interpreted to be the result of active transtensional or extensional tectonism throughout the area during the Devonian and early Carboniferous (Martina et al., 2018).

While there was synchronous deposition along both margins of the Paganzo Basin, there does not appear to have been any drainage connectivity between the two depocenters during the time of glaciation. Based on an extensive compilation of paleoflow directions from multiple studies, there appears to be a separation or pattern of flow directions (cf. Scalabrini Ortiz, 1972; Andreis et al., 1975; López-Gamundí and Amos, 1985; Buatois and Mángano, 1994; López-Gamundí et al., 1994; López-Gamundí and Martínez, 2000; Kneller et al., 2004; Henry et al., 2008; Alonso-Muruaga et al., 2011; Aquino et al., 2014; Valdez-Buso et al., 2017, 2020; Limarino et al., 2014; Fallgatter et al., 2019; Milana and di Pasquo, 2019, Fig. 12). Along the western margin, the flow directions indicate a more radial pattern away from a central area, from which a series of uplifted blocks, or elevated nucleation points, can be inferred (Fig. 12). Additionally, several studies along the Precordilleran region describe paleovalleys with depths of 1000–2500 m and filled with glacigenic and glacially influenced deposits up to 450 m thick (cf. Dykstra et al., 2006, 2007; Henry et al., 2008, 2010; Aquino et al., 2014; Valdez Buso et al., 2017, 2020; Milana and di Pasquo, 2019). This body of evidence seems to support the hypothesis that there existed a mountain belt or upland along the western margin of the Paganzo Basin, at least during the Serpukhovian-Bashkirian glaciation phase during the LPIA in Argentine Gondwana. Paleovalleys that are over 2.5 km deep, along with the radial distribution of paleoflow, indicate substantial relief in the Precordilleran region during the mid-Carboniferous. Such relief is characteristic is of a substantial upland rather than the occurrence of a gentle topographic arch.

9.1. Post-glacial sedimentation

Along the western margin of the basin, the basal diamictites of the Guandacol are replaced by shales interpreted as a flooding event, which corresponds to a post-glacial transgression that is recorded at several other localities across the Paganzo Basin (Limarino et al., 2002b, 2014; Marenssi et al., 2005; Net and Limarino, 2006; Pauls et al., 2019). The metamorphic and granitic clast lithologies from the post-glacial facies of the Guandacol Formation are interpreted to represent a more distal provenance (cf. Marenssi et al., 2005). Similar to our interpretation for the lower Guandacol Formation sample, we interpret these clasts as sourced from a location to the east of the Precordilleran Terrane, probably from the Sierra de Pie de Palo or Sierra Valle Fértil areas (cf. Pankhurst et al., 1998, 2000; Ramos et al., 1998, 2010, 2015; Rapela et al., 1998; Vujovich et al., 2004; Rapalini, 2005; Dahlquist et al., 2010; Sial et al., 2013; Verdecchia et al., 2011, 2014; Einhorn et al., 2015). The age peaks from the detrital zircon geochronology results correspond to the Mesoproterozoic ages found within the Sierra de Pie de Palo complex, as well as the Sierra de Maz and Umango ranges (Mesoproterozoic age ranges: 1000–1200 Ma; Varela et al., 2003, 2005; Vujovich et al., 2004; Naipauer et al., 2010a, 2010b, Figs. 10 and 11). The Ordovician ages correspond well with ages found in granites and gneisses from the Sierra de Valle Fértil (Cambrian-Ordovician age ranges: 500-450 Ma; Pankhurst et al., 2000). The age population range of the upper Guandacol Formation sample (CDH0923-3 S) indicates a drainage shift, or unroofing of basement material in an eastward direction, as proximal depositional environments prograde westward during the early Pennsylvanian (Limarino et al., 2002a, 2002b; 2006, 2014; Tedesco et al., 2010). Additionally, the youngest detrital zircon crystal analyzed in CDH0923-3 S (309 ± 11 Ma) may indicate a much younger age for the uppermost Guandacol Formation in this location than has been previously interpreted (cf. Gulbranson et al., 2010; César et al., 2011).

There is no record of striated pavements nor striated or faceted clasts in the Olta-Malanzán paleovalley, but that does not preclude a cold environment, with the occasional development of lake ice as there is evidence of potential ice-rafted debris. The lonestones could also have been from rock fall off of valley walls into the narrow paleovalley (cf. Moxness et al., 2018), as physical weathering and rock fall is prevalent in cold climate environments. Paleocurrent measurements at the base of the Malanzán Formation point to flow through the narrow paleovalley in a south-southwest direction. The large conglomeratic deltas of the upper Malanzán Formation at the interpreted paleomouth near the town of Malanzán indicate that paleoflow is to the west, but these deltas are considered to be post-glacial deposits, and therefore cannot be used to infer paleoflow from a glacier across the Paganzo Basin from east to west. Furthermore, the paleovalley narrows where tributary valleys connect with the main axis, and the paleoflow measurements follow the S-SW and lazy-S shape of the valley walls. This trend suggests internal and localized flow within a confined alpine valley setting subjected to tectonic activity (cf. Moxness et al., 2018) rather than a paleofjord or glacially-carved valley system.

9.2. Distinct depositional centers for the lower Paganzo Group strata

While the detrital zircon sample sets contain similar age peaks, there are distinguishing patterns between the two sample sets that warrants further comparative analysis. The similar age populations is not wholly unexpected based on the similarities in age suites of the igneous and metamorphic basement complexes found throughout the Paganzo Basin region (Figs. 10 and 11). The most important difference between the two formations, which provides clear evidence that these two localities do not share the same provenance, is the appearance of the Mesoproterozoic peaks in the Guandacol Formation samples, which point to a Cuyania terrane provenance. A second important distinction is the absence of early Carboniferous detrital zircons in the Guandacol Formation, and the presence of these ages within the Malanzán Formation, which indicates that an ice center did not drain from the eastern Sierras Pampeanas and across the Paganzo Basin. In addition to the provenance analysis, the evidence accumulated by the lithofacies and paleoflow analyses indicates that there were most likely separate depositional centers throughout the Paganzo Basin during the Visean and Serpukhovian-Bashkirian glaciations (Fig. 12).

Based on the evidence compiled here, there could not have been one ice sheet centered over the Sierras Pampeanas to the east of the Paganzo Basin, as was postulated in Hypothesis 2 (Fig. 2C). Instead, we propose a revision of Hypothesis 1 (Fig. 2B). As there is evidence of glaciation along the Protoprecordilleran region, there is a distinct lack of this evidence in the Sierras de Chepes and Los Llanos region. It is likely that there was a localized paleovalley system within the Sierras de Chepes and Los Llanos region during the deposition of the lower Malanzán Formation in the eastern Paganzo Basin region (Fig. 12). The region in the east was largely separated from the depositional system for the glacial diamictites of the lower Guandacol Formation, quite possibly by the uplifted blocks along the Famatina arch and Pie de Palo arch systems (Fig. 12). Further analyses are needed to further constrain glacial centers in the Protoprecordilleran and Sierra de Pie de Palo ranges, or if there were other glacial centers located in the Famatina arch system in the north-central region (Fig. 12).

10. Conclusions

Evidence supporting the presence of glaciers was identified along the western margin, specifically along the Protoprecordilleran mountain belt region. This evidence was noted based on the facies analyzed of the

Guandacol Formation at the Agua Hedionda anticline locality near Huaco. However, we found no evidence of glaciation from the facies of the Malanzán Formation located in the Sierra de Chepes region of the eastern Paganzo Basin. This body of evidence does not support the hypothesis (Hypothesis 2) that there was an ice sheet centered on the eastern Sierras Pampeanas to the east of the Paganzo Basin. Furthermore, the compiled paleoflow measurements indicate flow was distinct for the separate uplands across the region. At Huaco, glacial ice flowed toward the northwest (313°), which differs from the Olta-Malanzán paleovalley that had flow toward the south-southwest. This provides clear evidence that there were discrete glaciated uplands centered on the Protoprecordilleran fold-and-thrust belt, while the eastern Sierras Pampeanas remained unglaciated. In addition to the sedimentology and paleoflow measurements, the detrital zircon age populations for both localities suggest that there was more than one depositional center in the Paganzo Basin during the middle Carboniferous. There was one localized catchment for the Guandacol Formation at Huaco that drained westward off the Sierra de Pie de Palo or Sierra Valle Fértil. The strata at Olta-Malanzán paleovalley are sourced from the Sierra de Chepes and Los Llanos ranges, with a minor component source region further to the east. Our evidence refines the understanding of glacial extent across the Paganzo Basin and provides insight into a more complicated glaciation history along the western margin of South American Gondwana.

Author statement

I attest that all authors contributed significantly to the creation of this manuscript. I believe these individuals should be listed as authors because each of these individuals provided insight and assistance in the field and in the laboratory. Without their knowledge, this study would not have been possible. I confirm that the manuscript has been read and approved by all named authors. I confirm that the order of authors listed in the manuscript has been approved by all named authors.

The Corresponding Author declared on the title page of the manuscript is: Dr. Kathryn N Pauls. This author submitted this manuscript using his/her account in editorial submission system.

Declaration of competing interest

The authors declare that they have no known competing financial interests or personal relationships that could have appeared to influence the work reported in this paper.

Acknowledgements

Financial support for this study was provided by various grants from numerous agencies including the Geological Society of America, the Society for Sedimentary Geologists, the University of Wisconsin-Milwaukee Center for Latin American and Caribbean studies, the Wisconsin Geological Society, University of Wisconsin-Milwaukee (RGI grant), the University of Wisconsin-Milwaukee Department of Geosciences, the Universidad de Buenos Aires, CONICET, and grants from the USA National Science Foundation (Grants 1443557, 1559231, and 1729219).

Appendix A. Supplementary data

Supplementary data to this article can be found online at https://doi.org/10.1016/j.jsames.2020.102899.

References

Alonso-Muruaga, P.J., Limarino, C.O., Spalletti, L.A., Colombo Piñol, F., 2011. Findings of intraformational striated pavements in the Late Carboniferous glacial deposits of the Andean Precordillera, Argentina. Lat. Am. J. Sedimentol. Basin Anal. 18, 151–157.

Alonso-Muruaga, P.J., Limarino, C.O., Spalletti, L.A., Piñol, F.C., 2018. Depositional settings and evolution of a fjord system during the carboniferous glaciation in Northwest Argentina. J. S. Am. Earth Sci. 369, 28–45.

Anderson, R.S., Riihimaki, C.A., Safran, E.B., MacGregor, K.R., 2006. Facing reality: late Cenozoic evolution of smooth peaks, glacially ornamented valleys and deep river gorges of Colorado's Front Range. In: Willett, S.D., et al. (Eds.), Tectonics, Climate and Landscape Evolution, vol. 398. Special Papers Geological Society of America, pp. 397–418.

Andreis, R.R., Bossi, G.E., 1981. Algunos ciclos lacustres en la Formación Malanzán (Carbónico superior) en la región de Malanzán, sierra de Los Llanos, provincia de La Rioja [artículos de libros]. Public: 8o. Congreso Geológico Argentino. San Luis. Actas 4, 639–655.

Andreis, R.R., Spalletti, L.A., Mazzoni, M.M., 1975. Estudio geologico del subgrupo Sierra de Maz (Paleozoico Superior), Sierra de Maz, Provincia de La Rioja, República Argentina. Rev. Asoc. Geol. Argent. 30 (3), 247–273.

Andreis, R.R., Archangelsky, S., Leguizamón, R.R., 1986. El paleovalle de Malanzán: nuevos criterios para la estratigrafía del Neopaleozoico de la sierra de Los Llanos, La Rioja, República Argentina, vol. 57. Boletín de la Academia Nacional de Ciencias (Córdoba), pp. 1–119.

Aquino, C.D., Milana, J.P., Faccini, U.F., 2014. New glacial evidences at the Talacasto paleofjord (Paganzo basin, W-Argentina) and its implications for the paleogeography of the Gondwana margin. J. S. Am. Earth Sci. 56, 278–300.

Ashley, G.M., Shaw, J., Smith, N.D., 1985. Glacial Sedimentary Environments. SEPM Short Course No. 16. Society of Paleontologists and Mineralogists, Tulsa, OK, p. 246.

Astini, R.A., Benedetto, J.L., Vaccari, N.E., 1995. The Early Paleozoic evolution of the Argentine Precordillera as a Laurentian rifted, drifted and collided terrane: a geodynamic model. Geol. Soc. Am. Bull. 107, 253–273. https://doi.org/10.1130/0016-7606(1995)107<0253:TEPEOT>2.3.CO, 2.

Astini, R.A., Martina, F., Ezpeleta, M., Dávila, F.D., Cawood, P.A., 2009. Chronology from rifting to foreland basin in the Paganzo Basin (Argentina), and a reapprisal on the "eo- and neohercynian" tectonics along western Gondwana. In: XII Congreso Geológico Chileno, Santiago, Chile. Universidad de Chile, Santiago, Chile, pp. 1–4. Extended Abstracts S9 010.

Astini, R., 2010. Linked basins and sedimentary products across an accretionary margin: the case for the late history of the peri-Gondwanan Terra Australis orogen through the stratigraphic record of the Paganzo Basin. In: Papa, C., Astini, R. (Eds.), Field Excursion Guidebook, 18th International Sedimentological Congress. International Association of Sedimentologists, Mendoza, Argentina, p. 58.

Azcuy, C.A., 1975. Miosporas sel Namuriano y Westfaliano de la comarca de Malanzán-Loma Larga, provincia de La Rioja, Argentina. II, 12. Descripciones sistemáticas y significado estratigráfico de las microfloras, Ameghiniana, pp. 113–163.

Azcuy, C.L., Andreis, R.R., Cuerda, A., Hünicken, M.A., Pensa, M.V., Valencio, D.A., Vilas, J.F., Amos, A.J., Archangelsky, S., Berkowski, D.A., Leguizamón, R., 1987. Cuenca Paganzo. In: Archangelsky, S., Amos, A.J., Andreis, R., Azcuy, C.L., González, C.R., López-Gamundí, O., Sabattini, N. (Eds.), El sistema Carbonífero en la República Argentina. Academia Nacional De Ciencias, Córdoba, pp. 41–100.

Baird, D.M., 1962. Ripple marks. J. Sediment. Petrol. 32 (2), 332–334.

Basilici, G., Luca, P.H.V.d., Poiré, D.G., 2012. Hummocky cross-stratification-like structures and combined-flow ripples in the Punta Negra Formation (Lower-Middle Devonian, Argentine Precordillera): a turbiditic deep-water or storm-dominated prodelta inner-shelf system? Sediment. Geol. 267–268, 73–92.

Bennett, M.R., Doyle, P., Mather, A.E., Woodfin, J., 1994. Testing the climatic significance of dropstones: an example from the Miocene of the Sorbas Basin. south east Spain. Geology 131, 845–848.

Bhattacharya, J.P., 2006. Deltas. In: Posamentier, H., Walker, R.G. (Eds.), Facies Models Revisited, vol. 84. SEPM Special Publication, pp. 237–292.

Bossi, G., Andreis, R.R., 1985. Secuencias deltaicas y lacustres del Carbonifero del centro-oeste argentino. X International Congress on Carboniferous Stratigraphy and Geology, Madrid, pp. 285–309.

Boulton, G.S., 1990. Sedimentary and sea level changes during glacial cycles and their control on glacimarine facies architecture. In: Dowdeswell, J.A., Scourse, J.D. (Eds.), Glaciomarine Environments: Processes and Sediments, V. 53. Geological Society of London, Special Publications, pp. 15–52.

Bracaccini, I.O., 1948. Los Estratos de Paganzo y sus niveles plantiferos en la sierra de los Llanos (provincial de La Rioja). Rev. Asoc. Geol. Argent. 1, 19–61.

Buatois, L.A., Mángano, M.G., 1994. Lithofacies and depositional processes from a Carboniferous lake of Gondwana, Sierra de Narváez, northwest Argentina. Sediment. Geol. 93, 25–49. https://doi.org/10.1016/0037-0738(94)90027-2.

Buatois, L.A., Mángano, M.G., 1995. Post-glacial lacustrine event sedimentation in an ancient mountain setting: carboniferous Lake Malanzán (western Argentina). J. Paleolimnol. 14, 1–22.

Buatois, L.A., Netto, R.G., Mángano, M.G., 2010. Ichnology of late Paleozoic postglacial transgressive deposits in Gondwana: reconstructing salinity conditions in coastal ecosystems affected by strong meltwater discharge, 468. Geological Society of America Special Papers, pp. 149–173. https://doi.org/10.1130/2010.2468(07.

Caputo, M.V., Crowell, J.C., 1985. Migration of glacial centers across Gondwana during paleozoic era, 96. Geological Society of America Bulletin, pp. 1020–1036.

Caputo, M.V., de Melo, J.H.G., Streel, M., Isbell, J.L., 2008. Late devonian and early carboniferous glacial records of South America. In: Fielding, C.R., Frank, T.D., Isbell, J.L. (Eds.), Resolving the Late Paleozoic Ice Age in Time and Space. Geological Society of America Special Publication., Boulder, CO, pp. 161–173.

Casquet, C., Baldo, E., Pankhurst, R.J., Rapela, C.W., Galindo, C., Fanning, C.M., Saavedra, J., 2001. Involvement of the Argentine Precordillera Terrane in the Famatinian mobile belt: Geochronological (U–Pb SHRIMP) and metamorphic evidence from the Sierra de Pie de Palo. Geology 29, 703–706.

Casquet, C., Rapela, C.W., Pankhurst, R.J., Baldo, E.G., Galindo, C., Fanning, C.M., Dahlquist, J.A., Saavedra, J., 2012. A history of proterozoic terranes in southern south America: from rodinia to Gondwana. Geoscience Frontiers 3, 137–145. https://doi.org/10.1016/j.gsf.2011.11.004.

Césari, S.N., Limarino, C.O., Gulbranson, E.L., 2011. An Upper Paleozoic bio-chronostratigraphic scheme for the western margin of Gondwana. Earth Sci. Rev. 106, 149–160.

Colella, A., De Boer, P.L., Nio, S.D., 1987. Sedimentology of a marine intermontane pleistocene gilbert-type fan-delta complex in the crati basin. Calabria, southern Italy. Sedimentology 34, 721–736.

Craddock, J.P., Ojakangas, R.W., Malone, D.H., Konstantinou, A., Mory, A., Thomas, R.J., Craddock, S.D., Pauls, K.N., Zimmerman, U., Botha, G., Rocha-Campos, A., de Pazos, P.R., Tohver, E., Riccomini, Cl, Martin, J., Redfern, J., Horstwood, M., Gehrels, G., 2019. Provenance of permo-carboniferous diamictites across Gondwana. Earth Sci. Rev. https://doi.org/10.1016/j.earscirev.2019.01.01.

Crookshanks, S., Gilbert, R., 2008. Continuous, diurnally fluctuating turbidity currents in kluane lake, yukon territory. Can. J. Earth Sci. 45, 1123–1138.

Dahlquist, J.A., Alasino, P.H., Nelson Eby, G., Galindo, C., Casquet, C., 2010. Fault controlled Carboniferous A-type magmatism in the proto-Andean foreland (Sierras Pampeanas, Argentina): geochemical constraints and petrogenesis. Lithos 115, 65–81.

Dietrich, P., Franchi, F., Setlhabi, R.P., Bamford, M., 2019. The nonglacial diamictite of toutswemogala hill (lower karoo supergroup, Central Botswana): implications on the extent of the late paleozoic ice age in the kalahari-karoo basin. J. Sediment. Res. 89, 875–889. https://doi.org/10.2110/jsr.2019.48.

Drobe, M., Lopez de Luchi, M.G., Steenken, A., Frei, R., Naumann, R., Siegesmund, S., Wemmer, K., 2009. Provenance of the late proterozoic to early cambrian metaclastic sediments of the sierra de San Luis (eastern Sierras Pampeanas) and cordillera oriental, Argentina. J. S. Am. Earth Sci. 28, 239–262.

Drobe, M., López de Luchi, M., Steenken, A., Wemmer, K., Naumann, R., Frei, R., Siegesmund, S., 2011. Geodynamic evolution of the eastern Sierras Pampeanas (central Argentina) based on geochemical, Sm–Nd, Pb–Pb and SHRIMP data. Int. J. Earth Sciences 100, 631–657.

Dykstra, M., Kneller, B., Milana, J.P., 2006. Deglacial and postglacial sedimentary architecture in a deeply incised paleovalley–paleofjord — the Pennsylvanian (late Carboniferous) Jejenes Formation, San Juan, Argentina, 118. Geological Society of America Bulletin, pp. 913–937.

Dykstra, M., Kneller, B., Milana, J.P., 2007. A high-resolution record of deep-water processes in a confined paleofjord, quebrada de Las Lajas, Argentina. In: Nilsen, T.H., Shew, R.D., Steffens, G.S., Studlick, J.R.J. (Eds.), Atlas of Deep-Water Outcrops: AAPG Studies in Geology 56. CD-ROM, p. 19.

Dykstra, M., Garyfalou, K., Kertznus, V., Kneller, B., Milana, J.P., Molinaro, M., Szuman, M., Thompson, P., 2011. Mass-transport deposits: combining Outcrop studies and seismic forward modeling to understand lithofacies distributions, deformation and their seismic expression. In: Shipp, R.C., Weimer, P., Posamentier, H.W. (Eds.), Mass Transport Deposits in Deepwater Settings. 96. SEPM Special Publications, pp. 293–310.

Einhorn, J.C., Gehrels, G.E., Vernon, A., DeCelles, P.G., 2015. U-Pb zircon geochronology of Neoproterozoic–Paleozoic sandstones and Paleozoic plutonic rocks in the Central Andes (21°S–26°S). In: DeCelles, P.G., Ducea, M.N., Carrapa, B., Kapp, P.A. (Eds.), Geodynamics of a Cordilleran Orogenic System: the Central Andes of Argentina and Northern Chile, vol. 212. Geological Society of America Memoir, pp. 115–124. https://doi.org/10.1130/2015.1212(06).

Enkelmann, E., Ridgway, K.D., Carignano, C., Linnemann, U., 2014. A thermochronometric view into an ancient landscape: tectonic setting, and inversion of the Paleozoic eastern Paganzo basin. Argentina. Lithosphere 6, 93–107.

Enkelmann, E., Garver, J.I., 2015. Low-temperature thermochronology applied to ancient settings. J. Geodyn. 93, 17–30.

Eyles, C.H., Eyles, N., 2010. Glacial deposits. In: James, N.P., Dalrymple, R.W. (Eds.), Facies Models 4. GEOtext 6. Geological Association of Canada, St. John's, Newfoundland, pp. 73–104.

Fallgatter, C., Valdez Buso, V., Paim, P.S.G., Milana, J.P., 2019. Stratigraphy and depositional architecture of lobe complexes across a range of confinements: examples from the late Paleozoic Paganzo Basin, Argentina. Mar. Petrol. Geol. 110, 254–274. https://doi.org/10.1016/j.marpetgeo.2019.07.020.

Fielding, C.R., Frank, T.D., Isbell, J.L., 2008. The late Paleozoic ice age—a review of current understanding and synthesis of global climate patterns. In: Fielding, C.R., Frank, T.D., Isbell, J.L. (Eds.), Resolving the Late Paleozoic Ice Age in Time and Space, vol. 441. Geological Society of America Special Paper, pp. 343–354.

Gani, M.R., 2004. From turbid to lucid: a straightforward approach to sediment gravity flows and their deposits. Sediment. Rec. 2 (3), 4–8.

Gastaldo, R.A., DiMichele, W.A., Pfefferkorn, H.W., 1996. Out of the icehouse into the greenhouse: a late Paleozoic analogue for modern global vegetational change. GSA Today (Geol. Soc. Am.) 10, 1–7.

Gehrels, G.E., Valencia, V., Ruiz, J., 2008. Enhanced precision, accuracy, efficiency, and spatial resolution of U-Pb ages by laser ablation–multicollector–inductively coupled plasma–mass spectrometry. G-cubed 9, Q03017. https://doi.org/10.1029/2007GC001805.

Gehrels, G., 2011. Detrital zircon U-Pb geochronology: current methods and new opportunities. In: Busby, C., Azor, A. (Eds.), Recent Advances in Tectonics of Sedimentary Basins. Blackwell Publishing.

Gehrels, G., Pecha, M., 2014. Detrital zircon U-Pb geochronology and Hf isotope geochemistry of Paleozoic and Triassic passive margin strata of western Morth America. Geosphere 10, 49–65.

Gilbert, R., 1990. Rafting in glacimarine environments. In: Dowdeswell, J.A., Scourse, J. D. (Eds.), Glacimarine Environments: Processes and Sediments, vol. 53. Geological Society London Special Publications, pp. 105–120.

Godt, J.W., Coe, J.A., 2007. Alpine debris flows triggered by a 28 July 1999 thunderstorm in the central Front Range, Colorado. Geomorphology 84, 80–97.

Gonzalez Bonorino, G., 1975. Acerca de la existencia de la Protoprecordillera de cuyo. In: Actas. VI Congreso Geologico Argentino, vol. 1. Bahia Blanca, pp. 101–107.

Griffis, N.P., Mundil, R., Montañez, I.P., Isbell, J., Fedorchuk, N., Vesely, F., Iannuzzi, R., Qing-Zhu, Y., 2018. A new stratigraphic framework built on U-Pb single zircon TIMS ages with implications for the timing of the Penultimate Icehouse (Paraná Basin, Brazil). Earth Planet Sci. Lett.

Gulbranson, E.L., Montañez, I.P., Schmitz, M.D., Limarino, C.O., Isbell, J.L., Marenssi, S. A., Crowley, J.L., 2010. High-precision U–Pb calibration of Carboniferous glaciation and climate history, Paganzo Group, NW Argentina, 122. Geological Society of America Bulletin, pp. 1480–1498.

Gulbranson, E.L., Montañez, I.P., Tabor, N., Limarino, C.O., 2015. Late Pennsylvanian aridification on the southwestern margin of Gondwana (Paganzo Basin, NW Argentina): a regional expression of a global climate perturbation. Palaeogeogr. Palaeoclimatol. Palaeoecol. 417, 220–235.

Gutiérrez, P.R., Limarino, C.O., 2001. Palinologia de la Formacion malanzan (carbonifero superior), La rioja, Argentina;. nuevos datos y consideraciones paleoambientales: Ameghiniana 38 (1), 99–118.

Hambrey, M.J., Glasser, N.F., 2012. Discriminating glacier thermal and dynamic regimes in the sedimentary record. Sediment. Geol. 251–252, 1–33.

Henry, L.C., 2007. Carboniferous Glacigenic Deposits of the Hoyada Verde and Tramojo Formations of the Calingasta-Uspallata Basin, West Central Argentina. M.S. Thesis, University of Wisconsin-Milwaukee, p. 151.

Henry, L.C., Isbell, J.L., Limarino, C.O., 2008. Carboniferous glacigenic deposits of the Protoprecordillera of west central Argentina. In: Fielding, C.R., Frank, T.D., Isbell, J. L. (Eds.), Resolving the Late Paleozoic Ice Age in Time and Space, vol. 441. Geological Society of America Special Paper, pp. 131–142.

Henry, L.C., Isbell, J.L., Limarino, C.O., McHenry, L.J., Fraiser, M.L., 2010. Mid-Carboniferous deglaciation of the Protoprecordillera, Argentina, recorded in the Agua de Jagüel paleovalley. Palaeogeogr. Palaeoclimatol. Palaeoecol. 298, 112–129.

Holz, M., Souza, P.A., Iannuzzi, R., 2008. Sequence stratigraphy and biostratigraphy of the late carboniferous to early permian glacial succession (itarare subgroup) at the eastern-southeastern margin of the parana basin, 441. Special Paper - Geological Society of America, Brazil, pp. 115–129.

Huff, W.D., Davis, D., Bergström, S.M., Krekeler, M.P.S., Kolata, D.R., Cingolani, C.A., 1998. A biostratigraphically well-constrained K-bentonite U–Pb zircon age of the lowermost Darriwillian Stage (Middle Ordovician) from the Argentine Precordillera. Episodes 20, 29–33.

Isbell, J.L., Henry, L.C., Gulbranson, E.L., Limarino, C.O., Fraiser, M.L., Koch, Z.J., Ciccioli, P.L., Dineen, A.A., 2012. Glacial paradoxes during the late Paleozoic ice age: evaluating the equilibrium line altitude as a control on glaciation. Gondwana Res. 22, 1–19.

Jordan, T.E., Zeitler, P., Ramos, V., Gleadow, A.J.W., 1989. Thermochronometric data on the development of the basement peneplain in the Sierras Pampeanas, Argentina. J. S. Am. Earth Sci. 2 (3), 207–222.

Kay, S.M., Orrel, S., Abbruzzi, J.M., 1996. Zircon and whole rock Nd-Pb isotopic evidence for a Greenville age and Laurentian origin for the basement of the Precordillera terrane in Argentina. J. Geol. 104, 637–648.

Keller, M., 1999. Argentine Precordillera: sedimentary and plate tectonic history of a Laurentian crustal fragment in South America. Geol. Soc. Am. Spec. Pap. 341, 131. https://doi.org/10.1130/0-8137-2341-8.1.

Keller, M., Buggisch, W., Lehnert, O., 1998. The stratigraphical record of the Argentine Precordillera and its plate-tectonic background. In: Pankhurst, R.J., Rapela, C.W. (Eds.), The Proto-Andean Margin of Gondwana, vol. 142. Geological Society, London, Special Publications, pp. 35–56.

Kempema, E.W., Reimnitz, E., Barnes, P.W., 2001. Anchor-ice formation and ice rafting in southwestern Lake Michigan, U.S.A. J. Sediment. Res. 71, 346–354.

Kneller, B., Milana, J.P., Buckee, C., Al Ja'aidi, O.S., 2004. A depositional record of deglaciation in a paleofjord (Late Carboniferous [Pennsylvanian] of San Juan Province, Argentina): the role of catastrophic sedimentation, 116. Geological Society of America Bulletin, pp. 348–367.

Lambert, A., Giovanoli, F., 1988. Records of riverborne turbidity currents and indications of slope failures in the Rhone Delta of Lake Geneva. Limnol. Oceanogr. 33, 458–468.

Lawson, D.E., 1979. Sedimentological analysis of the western terminus región of the Matanuska Glacier, Alaska, 79–9. Cold Regions Research and Engineering Laboratory Report, p. 112.

Leal, P.R., Hartmann, L.A., Santos, J.O.S., Miró, R.C., Ramos, V.A., 2003. Volcanismo postorogénico en el extremo norte de las Sierras Pampeanas Orientales: Nuevos datos geocronológicos y sus implicancias tectónicas. Revista Asociación Geológica Argentina 58, 593–607.

Limarino, C., Gutiérrez, P., 1990. Diamictites in the Agua Colorada Formation (northwestern Argentina); new evidence of Carboniferous glaciation in South America. J. S. Am. Earth Sci. 3 (1), 9–20.

Limarino, C.O., Marenssi, S.A., Tripaldi, A., Caselli, A.T., 2002a. Evolution of the Upper Paleozoic basins of western Argentina during the maximum extent of Gondwana. 16th International Sedimentological Congress, Abstracts, pp. 224–225.

Limarino, C.O., Césari, S.N., Net, L.I., Marenssi, S.A., Gutiérrez, P.R., Tripaldi, A., 2002b. The Upper Carboniferous postglacial transgression in the Paganzo and Río Blanco Basins (northwestern Argentina): facies and stratigraphic significance. J. S. Am. Earth Sci. 15, 445–460.

Limarino, C.O., Spalletti, L.A., 2006. Paleogeography of the Upper Paleozoic basins of southern South America: an overview. J. S. Am. Earth Sci. 22, 134–155.

Limarino, C.O., Tripaldi, A., Marenssi, S., Fauqué, L., 2006. Tectonic, sea level, and climatic controls on late Paleozoic sedimentation in the western basins of Argentina. J. S. Am. Earth Sci. 33, 205–226.

Limarino, C.O., Césari, S.N., Spalleti, L.A., Taboada, A.C., Isbell, J.L., Geuna, S., Gulbranson, E.L., 2014. A paleoclimatic review of southern South America during the late Paleozoic; A record from icehouse to extreme greenhouse conditions. Gondwana Res. 25, 1396–1421.

Llambías, E.J., Gregori, D., Basei, M.A., Varela, R., Prozzi, C., 2003. Ignimbritas riolíticas neoproterozoicas en la Sierra Norte de Córdoba: ¿evidencia de un arco magmático temprano en el ciclo Pampeano? Revista Asociación Geológica Argentina 58 (4), 572–582.

López-Gamundí, O.R., 1987. Depositional models for the glaciomarine sequences of Andean late Paleozoic basins of Argentina. Sediment. Geol. 52, 109–126.

López-Gamundí, O.R., Espejo, I.S., Conaghan, P.J., Powell, C.McA., Veevers, J.J., 1994. Southern South America. In: Veevers, J.J., Powell, C.McA. (Eds.), Permian–Triassic Pangean Basins and Foldbelts along the Panthalassan Margin of Gondwanaland. Geological Society of America Memoir 184, Boulder, Colorado, pp. 281–329.

López Gamundí, O.R., 1997. Glacial–postglacial transition in the late Paleozoic basins of southern South America. In: Martini, I.P. (Ed.), Late Glacial and Postglacial Environmental Changes: Quaternary, Carboniferous–Permian, and Proterozoic. Oxford University Press, Oxford, UK, pp. 147–168.

López-Gamundí, O.R., Amos, A.J., 1985. Consideraciones paleoambientales de las secuencias carbónicas del sector Precordillerano de la Cuenca Calingasta-Uspallata, San Juan y Mendoza: Primeras Jornadas sobre Geología de la Precordillera, Serie "A" Monografías y Reuniones, Asociacíon Geológica Argentina. Acta (2), 289–294.

López-Gamundí, O.R., Martínez, M., 2000. Evidence of glacial abrasion in the Calingasta–Uspallata and western Paganzo Basins, mid-Carboniferous of western Argentina. Palaeogeogr. Palaeoclimatol. Palaeoecol. 159, 145–165.

Ludwig, K.R., 2012. Isoplot 3.75. In: A Geochronological Toolkit for Excel, vol. 5. Berkeley Geochronology Center Special Publication, p. 75.

MacGregor, K.R., Anderson, R.S., Anderson, S.P., Waddington, E.D., 2000. Numerical simulations of glacial-valley longitudinal profile evolution. Geology 28, 1031–1034.

Marenssi, S.A., Limarino, C.O., Césai, S.N., Tripaldi, A., Caselli, A.T., 2002. Glacial and Postglacial Sedimentation in Western Paganzo Basin, Northwest Argentina. In: 16th International Sedimentological Congress, pp. 236–237. Abstracts, Johannesburg.

Marenssi, S.A., Tripaldi, A., Limarino, C.O., Caselli, A.T., 2005. Facies and architecture of a Carboniferous grounding-line system from the Guandacol Formation, Paganzo Basin, northwestern Argentina. Gondwana Res. 8, 187–202.

Martina, F., Canelo, H.N., Dávila, F.M., Hollanda, M.H.B.M., Teixeira, W., 2018. Mississippian lamprphyre dikes in western Sierras Pampeanas, Argentina: Evidence of transtensional tectonics along the SW margin of Gondwana. J. S. Am. Earth Sci. 83, 68–80.

Martinsen, O.J., 1990. Fluvial, inertia-dominated deltaic deposition in the Namurian (Carboniferous) of northern England. Sedimentology 37, 1099–1113.

Martínez, M., 1993. Hallazgo de fauna marina en la Formación Guandacol (Carbonífero) en la localidad de Agua Hedionda, San Juan, Precordillera Nororiental, Argentina. In: Compte Rendus XII Congrès International de la Stratigraphie et Gèologie du Carbonifère et Permien, vol. 2, pp. 291–296.

McKay, M.P., Weislogel, A.L., Jackson Jr., W.T., Dean, J., Fildani, A., 2018. Structural and magmatic controls on the turbidites of the Karoo Basin, South Africa. In: Ingersoll, R.V., Graham, S.A., Lawton, T.F. (Eds.), Tectonics, Sedimentary Basins, and Provenance: A Celebration of William R. Dickinson's Career. Geological Society of America Special Paper 540, pp. 689–705.

Milana, J.P., 1988. Sedimentacion estuarica carbonífera tardía en la Precordillera central, San Juan, Argentina. 2 Reunion Argent. Sedimentol, Buenos Aires, pp. 185–188. Actas.

Milana, J.P., Berscowski, F., 1987. Rasgos erosivos y depositacionales glaciales en el neopaleozoico de la precordillera central, San Juan, Argentina. 4a Reun. In: Internac. Work.Roup PICG-211. (IUGS-UNESCO), St. Cruz Sierra, Bolivia, Abstracts, pp. 46–48.

Milana, J.P., Bercowski, F., 1990. Facies y geometría de depositos glaciales en un paleovalle Carbonífero de Precordillera Central, San Juan, Argentina, 3 Reunioon Argentina de Sedimentología (San Juan). Actas, pp. 199–204.

Milana, J.P., Bercowski, F., 1993. Late Palaeozoic Glaciation in Paganzo Basin, Western Argentina: Sedimentological Evidence. Comptes Rendus XII ICC-P, Bs. As 1, 325–335.

Milana, J.P., Bercowski, F., Lech, R.R., 1987. Análisis de una secuencia marinocontinental Neopaleozoica en la región del Río San Juan, Precordillera Central, San Juan. In: 10th Cong. Geológ. Argent., Tucumán, Argentina, Actas III, pp. 113–116.

Milana, J.P., di Pasquo, M.M., 2019. New chronostratigraphy for a Lower to Upper Carboniferous strike-slip basin of W-Precordillera (Argentina): its paleogeographic, tectonic and glacial importance. J. S. Am. Earth Sci. 96 https://doi.org/10.1016/j.jsames.2019.102383.

Montañez, I.P., Tabor, N.J., Niemeier, D., DiMichele, W.A., Frank, T.D., Fielding, C.R., Isbell, J.L., Birgenheir, L.P., Rygel, M.C., 2007. CO2-forced climate and vegetative instability during late Paleozoic deglaciation. Science 315, 87–91.

Montañez, I.P., Poulsen, C.J., 2013. The late Paleozoic ice age: An evolving paradigm, 24 Annu. Rev. Earth Planet Sci. 41, 1–24.

Montanez, I.P., McElwain, J.C., Poulsen, C.J., White, J.D., DiMichele, W.A., Wilson, J.P., Griggs, G., Hren, M.T., 2016. Climate, pCO_2 and terrestrial carbon cycle linkages during late Palaeozoic glacial-interglacial cycles. Nat. Geosci. 9 (11), 824–828.

Montgomery, D.R., 2000. Valley formation by fluvial and glacial erosion. Geology 30 (11), 1047–1050.

Mottin, T.E., Vesely, F.F., Rodrigues, M.C.N.L., Kipper, F., Souza, P.A., 2018. The paths and timing of late Paleozoic ice revisited: New stratigraphic and paleo-ice flow interpretations from a glacial succession in the upper Itararé Group (Paraná Basin, Brazil). Palaeogeogr. Palaeoclimatol. Palaeoecol. 490, 488–504. https://doi.org/10.1016/j.palaeo.2017.11.031.

Moxness, L.D., Isbell, J.L., Pauls, K.N., Limarino, C.O., Schencman, J., 2018. Sedimentology of the mid-Carboniferous fill of the Olta paleovalley, eastern Paganzo Basin, Argentina: Implications for glaciation and controls on diachronous deglaciation in western Gondwana during the late Paleozoic Ice Age. J. S. Am. Earth Sci. 84, 127–148. https://doi.org/10.1016/j.jsames.2018.03.015.

Mulder, T., Alexander, J., 2001. The physical character of subaqueous sedimentary density flows and their deposits. Sedimentology 48, 269–299.

Naipauer, M., Vujovich, G.I., Cingolani, C.A., McClelland, W.C., 2010a. Detrital zircon analysis from the Neoproterozoic-Cambrian sedimentary cover (Cuyania terrane), Sierra de Pie de Palo, Argentina: evidence of a rift and passive margin system? J. S. Am. Earth Sci. 29, 306–326.

Naipauer, M., Cingolani, C.A., Vujovich, G.I., Chemale Jr., F., 2010b. Geochemistry of Neoproterozoic-Cambrian metasedimentary rocks of the Caucete Group, Sierra de Pie de Palo, Argentina: Implications for their provenance. J. S. Am. Earth Sci. 30, 84–96. https://doi.org/10.1016/j.jsames.2010.03.002.

Nemec, W., 1990. Aspects of sediment movement on steep delta slopes. In: Colella, A., Pior, D.B. (Eds.), Coarse-grained Deltas. IAS. Special Publication 10, pp. 29–73.

Net, L.I., 1999. Petrografía, diagénesis y procedencia de areniscas de la sección inferior del Grupo Paganzo (carbonífero) en la cuenca homónima. PhD Thesis, Universidad de Buenos Aires, p. 49.

Net, L.I., Limarino, C.O., 1999. Paleogeografía y correlación estratigráfica del Paleozoico Tardío de la Sierra de Los Llanos, provincia de La Rioja, Argentina. Rev. Asoc. Geol. Argent. 54 (3), 229–239.

Net, L.I., Alonso, M.S., Limarino, C.O., 2002. Source rock and environmental control on clay mineral associations, lower section of Paganzo group (Carboniferous), northwest Argentina. Sediment. Geol. 152, 183–199.

Net, L.I., Limarino, C.O., 2006. Applying sandstone petrofacies to unravel the Upper Carboniferous evolution of the Paganzo Basin, northwest Argentina. J. S. Am. Earth Sci. 22, 239–254.

Ottone, E.G., Holfeltz, G.D., Albanesi, G.L., Ortega, G., 2001. Chitinozoans from the Ordovician Los Azules Formation, Central Precordillera, Argentina. Micropaleontology 47, 97–110.

Pankhurst, R.J., Rapela, C.W., Saavedra, J., Baldo, E., Dahlquist, J., Pascua, I., Fanning, C.M., 1998. The Famitinian magmatic arc in the Central Sierras Pampeanas: An early to mid-Ordovician continental arc on the Gondwana margin. In: Pankhurst, R.J., Rapela, C.W. (Eds.), The Proto-Andean Margin of Gondwana, vol. 142. Geological Society of London Special Publication, pp. 343–367.

Pankhurst, R.J., Rapela, C.W., Fanning, C.M., 2000. Age and origin of coeval TTG, I- and S-type granites in the Famatinian belt of NW Argentina. Earth and Environmental Science Transactions of the Royal Society of Edinburgh 91, 151–168.

Pauls, K.N., Isbell, J.L., McHenry, L., Limarino, C.O., Moxness, L.D., Schencman, L.J., 2019. A paleoclimatic reconstruction of the Carboniferous-Permian paleovalley fill in the Eastern Paganzo Basin: Insights into glacial extent and deglaciation of southwestern Gondwana. J. S. Am. Earth Sci. 95 https://doi.org/10.1016/j.jsames.2019.102236.

Pazos, P.J., 2000. Análisis litofacial y trazas f6siles de las Formaciones Guandacol y Tupe. In: en el Ambit0 Occidental de la Cuenca Paganzo. Unpub. PhD Thesis, Univ. Buenos Aires, , Buenos Aires, Argentina, p. 467p.

Pazos, P.J., 2002a. The Late Carboniferous glacial to postglacial transition: facies and sequence stratigraphy, western Paganzo Basin, Argentina. Gondwana Res. 5, 467–487.

Pazos, P.J., 2002b. Palaeoenvironmental framework of the glacial-postglacial transition (Late Paleozoic) in the Paganzo-Calingasta Basin (southern South America) and the Great Karoo-Kalahari Basin (southern Africa): ichnological implications. Gondwana Res. 5, 619–640.

Postma, G., Nemec, W., Kleinspehn, K.L., 1988. Large floating clasts in turbidites: a mechanism for their emplacement. Sediment. Geol. 58, 47–61.

Powell, R.D., 1984. Glacimarine processes and inductive lithofacies modeling of ice shelf and tidewater glacier sediments based on Quaternary examples. Mar. Geol. 57, 1–52.

Powell, R.D., Cowan, E.A., 1986. Depositional processes at McBride Inlet and Riggs glacier. In: Anderson, P.G., Goldthwait, R.P., McKenzie, G.D. (Eds.), Observed Processes of Glacial Deposition in Glacier Bay, vol. 256. Ohio State University, Institute of Polar Studies, Miscellaneous Publications, Alaska, pp. 140–156.

Powell, R.D., Cooper, J.M., 2002. A glacial sequence stratigraphic model for temperate, glaciated continental shelves. In: Dowdeswell, J.A., Ó Cofaigh, C. (Eds.), Glacier-influenced Sedimentation on High-Latitude Continental Margins. Geological Society of London Special Publication 203, pp. 215–244.

Powell, R.D., Domack, E.W., 2002. Modern glacimarine environments. In: Menzies, J. (Ed.), Modern and Past Glacial Environments. Butterworth-Heinemann Ltd., Oxford, pp. 361–389.

Rabassa, J., Carignano, C., Cioccale, M., 2014. A general overview of Gondwana landscapes in Argentina. In: Rabassa, J., Ollier, C. (Eds.), Gondwana Landscapes in Southern South America: Argentina, Uruguay and Southern Brazil. Springer Earth System Science, Dordrecht, Heidelberg, New York, London, pp. 201–245.

Ramos, V., Jordan, T., Allmendinger, R., Kay, S., Cortés, J., Palma, M., 1984. Chilenia: un terreno alóctono en la evolución paleozoica de los Andes Centrales. In: 10° Congr. Geol, vol. 2. Actas, Argentino, pp. 84–106.

Ramos, V.A., 1988. Tectonics of the Late Proterozoic–Early Paleozoic: a collisional history of Southern South America. Episodes 11, 168–174.

Ramos, V.A., Dallmeyer, D., y Vujovich, G., Pankhurst, R., Rapela C, y, 1998. Time constraints on the Early Paleozoic docking of the Precordillera, Central Argentina. In: The Proto-Andean Margin of Gondwana, vol. 142. Geological Society, London, Special Publication, pp. 143–158.

Ramos, V.A., 1999. Evolución tectónica de la Argentina. In: Rasgos Estructurales del Territorio Argentino, vol. 29. Instituto de Geología y Recursos Minerales, Geología Argentina Anales, pp. 715–784, 24.
Ramos, V.A., 2000. The southern central Andes. In: Cordani, U.G., Milani, E.J., Thomaz Filho, A., Campos, D.A. (Eds.), International Geological Congress Rio de Janeiro, vol. 31. Tectonic evolution of South America, pp. 561–604.
Ramos, V.A., 2008. The basement of the Central Andes: the Arequipa and related terranes. Annu. Rev. Earth Planet Sci. 36, 289–324.
Ramos, V.A., Vujovich, G., Martino, R., Otamendi, J., 2010. Pampia: a large cratonic block missing in the Rodinia supercontinent. J. Geodyn. 50, 243–255.
Ramos, V.A., Escayola, M., Leal, P., Pimentel, M.M., Santos, J.O.S., 2015. The late stages of the Pampean Orogeny, C_ordoba (Argentina): Evidence of postcollisional Early Cambrian slab break-off magmatism. J. S. Am. Earth Sci. 64, 351–364. https://doi.org/10.1016/j.jsames.2015.08.002.
Rapalini, A.E., 2005. The accretionary history of southern South America from the latest Proterozoic to the late Paleozoic: Some paleomagnetic constraints. In: Vaughan, A.P. M., Leat, P.T., Pankhurst, R.J. (Eds.), Terrane Processes at the Margins of Gondwana, vol. 246. Geological Society London Special Publication, pp. 305–328.
Rapela, C.W., Pankhurst, R.J., Casquet, C., Baldo, E., Saavedra, J., Galindo, C., Fanning, C.M., 1998. The Pampean orogeny of the southern proto-Andes: evidence for Cambrian continental collision in the Sierras de Córdoba. In: Pankhurst, R.J., Rapela, C.W. (Eds.), The Proto-Andean Margin of Gondwana. Geological Society of London, pp. 181–217.
Rapela, C.W., Pankhurst, R.J., Baldo, E., Casquet, C., Galindo, C., Fanning, C.M., Saavedra, J., 2001. Ordovician metamorphism in the Sierras Pampeanas: New U-Pb SHRIMP ages in Central-East Valle Fértil and the Velasco Batholith. III Simposio Sudamericano de Geología Isotópica (III SSAGI). Publicación en CD-ROM.
Rapela, C.W., Pankhurst, R.J., Casquet, C., Fanning, C.M., Baldo, E.G., González-Casado, J.M., Galindo, C., Dahquist, J., 2007. The Río de la Plata craton and the assembly of SW Gondwana. Earth Sci. Rev. 83, 49–82.
Rapela, C.W., Pankhurst, R.J., Casquet, C., Dahlquist, J.A., Fanning, M., Baldo, E.G., Galindo, C., Alasino, P.H., Ramacciotti, C.D., Verdecchia, S.O., Murra, J.A., Basei, M. A.S., 2018. A review of the Famatinian Ordovician magmatism in southern South America: evidence of lithosphere reworking and continental subduction in the early proto-Andean margin of Gondwana. Earth Sci. Rev. 187, 259–285.
Reineck, H.E., Singh, I.B., 1980. Depositional Sedimentary Environments. Springer-Verlag, Berlin, p. 551.
Rocha Campos, A.C., dos Santos, P.R., Canuto, J.R., 2008. Late Paleozoic glacial deposits of Brazil; Parana Basin. In: Fielding, C.R., Frank, T.D., Isbell, J.L. (Eds.), Resolving the Late Paleozoic Ice Age in Time and Space, vol. 441. Geological Society of America Special Paper, pp. 97–114.
Sato, A.M., González, P.D., Sato, K., 2001. First indication of Mesoproterozoic age from the western basement of the Sierra de San Luis, Argentina, 3rd South American Symposium on Isotope Geology, Extended Abstracts (CD edition). Soc. Geol. Chile, Santiago, pp. 64–67.
Sato, A.M., González, P.D., Basei, M.A.S., Llambías, E.J., 2006. U-Pb ages of Komatiitic Rocks from Sierra de San Luis, Argentina. 5th SSAGI, Short Papers, pp. 169–173.
Scalabrini Ortiz, J., 1972. El Carbónico en el sector septentrional de la Precordillera Sanjuanina: Revista Asociacíon Geológica Argentina, vol. 27, pp. 351–377.
Schatz, E.R., Mángano, M.G., Buatois, L.A., Limarino, C.O., 2011. Life in the late Paleozoic ice age: Trace fossils from glacially influenced deposits in a late Carboniferous fjord of western Argentina. J. Paleontol. 85 (3), 502–518.
Sial, A.N., Peralta, S., Gaucher, C., Toselli, A.J., Ferreira, V.P., Frei, R., Parada, M.A., Pimentel, M.M., Pereira, N.S., 2013. High-resolution stable isotope stratigraphy of the upper Cambrian and Ordovician in the Argentine Precordillera: Carbon isotope excursions and correlations. Gondwana Res. 24, 330–348.
Sircombe, K.N., Stern, R.A., 2002. An investigation of artificial biasing in detrital zircon U-Pb geochronology due to magnetic separation in sample preparation. Geochem. Cosmochim. Acta 66 (13), 2379–2397.
Socha, B.J., Carignano, C., Rabassa, J., Mickelson, D.M., 2014. Gondwana glacial paleolandscape, diamictite record of Carboniferous valley glaciation, and preglacial remnants of an ancient weathering front in northwestern Argentina. In: Rabassa, J., Ollier, C. (Eds.), Gondwana Landscapes in Southern South America. Springer, Dordrecht, pp. 331–363.
Sohn, Y.K., 2000. Depositional processes of submarine debris flows in the Miocene fan deltas, Pohang Basin, SE Korea with special reference to flow transformation. J. Sediment. Res. 70, 491–503.
Sterren, A.F., Martínez, M., 1996. El paleovalle de Olta (Carbonífero): paleoambientes y paleogeografía. 13° Congreso Geológico Argentino y 3° Congreso Exploración de Hidrocarburos (Buenos Aires), Actas 2, 89–103.
Stanley, K.O., Surdam, R.C., 1978. Sedimentation on the front of Eocene Gilbert-type deltas, Washakie Basin, Wyoming. J. Sediment. Petrol. 48, 557–573.
Stuart-Smith, P.G., Camacho, A., Sims, J.P., Skirrow, R.G., Pieters, P.E., Black, L.P., Miró, R., 1999. U–Pb, Th–Pb and Ar–Ar geochronology from the southern, 1999. Uranium– Lead dating of felsic magmatic cycles in the southern Sierras Pampeanas, Argentina: implications for the tectonic development of the proto-Andean Gondwana margin. Laurentia Gondwana connections before Pangea. In: Ramos, V.A., Keppe, I. D. (Eds.), 336. Geological Society of America, Special Paper, pp. 87–114.
Talling, P.J., 2014. On the triggers, resulting flow types and frequencies of subaqueous sediment density flows in different settings. Mar. Geol. 352, 155–182.
Talling, P.J., Masson, D.G., Sumner, E.J., Malgesini, G., 2012. Subaqueous sediment density flows: Depositional processes and deposit types. Sedimentology 59, 1937–2003.
Tedesco, A., Ciccioli, P., Suriano, J., Limarino, C., 2010. Changes in the architecture of fluvial deposits in the Paganzo Basin (Upper Paleozoic of San Juan Province): an example of sea level and climatic controls on the development of coastal fluvial environments. Geol. Acta.
Thomas, G.S.P., Connell, R.J., 1985. Iceberg drop, dump, and grounding structures from Pleistocene glacio-lacustrine sediments, Scotland. J. Sediment. Petrol. 55 (2), 243–249.
Thomas, W.A., Astini, R.A., Mueller, P.A., McClelland, W.C., 2015. Detrital-zircon geochronology and provenance of the Ocloyic synorogenic clastic wedge, and Ordovician accretion of the Argentine Precordillera terrane. Geosphere 11 (6), 1749–1769. https://doi.org/10.1130/GES01212.1.
Toselli, A.J., Basei, M.A., Rossi de Toselli, J.N., Rudas, R., 2003. Análisis geoquímico-geocronológico de rocas granulíticas y calcosilicáticas de las Sierras Pampeanas Noroccidentales. Rev. Asoc. Geol. Argent. 58 (4), 629–642.
Valdez Buso, V., Pasquo, M.D., Milana, J.P., Kneller, B., Fallgatter, C., Chemale, F.J., Paim, P.S.G., 2017. Integrated U-Pb zircon and palynological/palaeofloristic age determinations of a Bashkirian palaeofjord fill, Quebrada Grande (Western Argentina). J. S. Am. Earth Sci. 73, 202–222.
Valdez Buso, V., Milana, J.P., di Pasquo, M., Paim, P.S.G., Philipp, R.P., Aquino, C.A., Cagliari, J., Junior, F.C., Kneller, B., 2020. Timing of the Late Paleozoic glaciation in western Gondwana: New ages and correlations from Paganzo and Paraná basins. Palaeogeogr. Palaeoclimatol. Palaeoecol. 544 https://doi.org/10.1016/j.palaeo.2020.109624.
Van Steijn, H., 1996. Debris-flow magnitude—frequency relationships for mountainous regions of Central and Northwest Europe. Geomorphology 15, 259–273.
Varela, R., Basei, M.A.S., Sato, A.M., González, P.D., Siga Jr., O., Campos Neto, M.C., Cingloani, C.A., 2003. Grenvillian basement and Famatinian events of the Sierra de Umango (29°S): A review and new geochronological data. IV South American Symposium on Isotope Geology- Short Papers, pp. 304–306.
Verdecchia, S.O., Casquet, C., Baldo, E.G., Pankhurst, R.J., Rapela, C.W., Fanning, M., Galindo, C., 2011. Mid- to Late Cambrian docking of the Río de la Plata Craton to southwestern Gondwana; age constraints from U-Pb SHRIMP detrital zircon ages from Sierras de Ambato and Velasco (Sierras Pampeanas, Argentina). Journal of the Geological Society of London 168, 1061–1071.
Verdecchia, S.O., Murra, J.A., Baldo, E.G., Casquet, C., Pascua, I., Saavedra, J., 2014. Geoquímica de las rocas metasedimentarias del Cámbrico medio al Ordovícico temprano de la Sierra de Los Llanos (Sierras Pampeanas, Argentina): Fuente de sedimentos, correlación y ambiente geotectónico. Andean Geol. 41 (2), 380–400. https://doi.org/10.5027/andgeoV41n2-a06.
Vesely, F.F., Rodrigues, M.C.N.L., da Rosa, E.L.M., Amato, J.A., Trzaskos, B., Isbell, J.L., Fedorchuk, N.D., 2018. Recurrent emplacement of non-glacial diamictite during the late Paleozoic ice age. Geology 46 (7), 615–618.
Visser, J.N.J., 1983. The problems of recognizing ancient sub- aqueous debris flow deposits in glacial sequences, 86. Transactions of the Geological Society of South Africa, pp. 127–135.
Vujovich, G.I., Ostera, H.A., 2003. Evidencias del ciclo Pampeano en el basamento del sector noroccidental de la sierra de San Luis. Rev. Asoc. Geol. Argent. 58 (4), 541–548.
Vujovich, G.I., Van Staal, C.R., Davis, W., 2004. Age constraints and the tectonic evolution and provenance of the Pie de Palo Complex, Cuyania composite terrane, and the Famatinian orogeny in the Sierra de Pie de Palo, San Juan, Argentina. Gondwana Res. 7, 1041–1056.
Willner, A.P., Gerdes, A., Massonne, H.-J., 2008. History of crustal growth and recycling at the Pacific convergent margin of South America at latitudes 29° -36° S revealed by a U-Pb and Lu-Hf isotope study of detrital zircon from late Paleozoic accretionary systems. Chem. Geol. 253, 114–129. https://doi.org/10.1016/j.chemgeo.2008.04.016.
Winsemann, J., Asprion, U., Meyer, T., Schramm, C., 2007. Facies characteristics of Middle Pleistocene (Saalian) ice-margin subaqueous fan and delta deposits, glacial Lake Leine, NW Germany. Sediment. Geol. 193, 105–129.